The role of climate-fuel feedbacks on Holocene biomass burning in upper-montane Carpathian forests

Vachel Carter, Přemysl Bobek, Alice Moravcová, Anna Šolcová, Richard Chiverrell, Jennifer Clear, Walter Finsinger, Angelica Feurdean, Ioan Tanţău, Enikő Magyari, et al.

The role of climate-fuel feedbacks on Holocene biomass burning in upper-montane Carpathian forests

Authors- Vachel A. Carter[1]*, Přemysl Bobek[2], Alice Moravcová[1], Anna Šolcová[1,2], Richard C. Chiverrell[3], Jennifer L. Clear[4,5], Walter Finsinger[6], Angelica Feurdean[7,8,9], Ioan Tanţău[9], Enikő Magyari[10, 11, 12], Tom Brussel[13], Petr Kuneš[1]

[1] Department of Botany, Faculty of Science, Charles University, Prague, Czech Republic

[2] Institute of Botany, The Czech Academy of Sciences, Průhonice, Czech Republic

[3] Department of Geography and Planning, University of Liverpool, Liverpool, United Kingdom

[4] Department of Geography and Environmental Science, Liverpool Hope University, Liverpool, United Kingdom

[5] Department of Forest Ecology, Czech University of Life Sciences, Prague, Czech Republic

[6] ISEM, University Montpellier, CNRS, EPHE, IRD, Montpellier, France

[7] Department of Physical Geography, Goethe University, Altenhöferallee 1, 60438 Frankfurt am Main, Germany,

[8] Senckenberg Biodiversity and Climate Research Centre (BiK-F), Senckenberganlage, 25, 60325, Frankfurt am Main, Germany

[9] Department of Geology, Babeş-Bolyai University, 400084 Cluj-Napoca, Romania

[10] Department of Environmental and Landscape Geography, Eötvös Loránd University, Budapest, Hungary

[11] MTA-MTM-ELTE Research Group for Paleontology, Budapest, Hungary

[12] GINOP Sustainable Ecosystems Group, MTA Centre for Ecological Research, Tihany, Hungary

[13] Department of Geography, University of Utah, Salt Lake City, Utah, USA

Correspondence:

Dr. Vachel A. Carter

vachel.carter@gmail.com

Revised manuscript for Global and Planetary Change

Highlights

- First high-resolution Holocene fire record from the High Tatra Mountains, Western Carpathians.
- Biomass burning in upper-montane Carpathian forests is influenced by forest composition and forest density, both of these are strongly-dependent on climate.
- Despite the reduced risk of fire implicit in *Picea abies* forests, biomass burning continued in forests with an intermediate forest cover, while fires with too dense of forest cover experienced less biomass burning.
- Future climate change may create a positive climate-fuel feedback, linking upper-montane forests with more *Pinus* cover to biomass burning.

Abstract

Over the past few decades, mean summer temperatures within the Carpathian Mountains have increased by as much as 2 ^{o}C leading to a projected increased forest fire risk. Currently, there are

no paleofire records from the Western Carpathians that provide the long-term range of natural variability to contextualise the response of upper-montane forests to future environmental change and disturbance regimes. We present the first high-resolution Holocene fire history record from the upper-montane ecotone from the High Tatra Mountains, Slovakia, as well as provide a regional synthesis of pan-Carpathian drivers of biomass burning in upper-montane forests. Our results illustrate that forest composition and density both greatly influence biomass burning in these hotspots for biodiversity, creating two different climate-fuel feedbacks. First, warmer conditions occurred in the early Holocene, coupled with generally higher abundances of *Pinus* sp., either *P. cembra* and *P. mugo*, created a positive climate-fuel relationship that resulted in higher amounts of biomass burning. Second, cooler and wetter late Holocene conditions led to denser *Picea abies* upper-montane forests, creating a negative climate-fuel feedback that reduced biomass burning in upper-montane forests across the Carpathians. Given that warmer and drier conditions are expected across the entire Carpathian region in the future, our results illustrate how future climate change could potentially create a positive climate-fuel relationship within upper-montane forests dominated by *Picea abies* and *Pinus cembra* and/or *P. mugo*.

Keywords

Fire; Upper-montane; Carpathians; Holocene; Sedimentary charcoal; Pollen; Macrofossils; *Picea abies*; forest composition; forest density

1 Introduction

Mountain forests are important ecosystems providing an array of ecosystem goods and services, with roughly half of the global human population depending upon these services

(Körner and Ohsawa, 2005). Mountain forests are also key hotspots for biodiversity, with higher levels of endemic richness as a result of high environmental heterogeneity and geographic isolation (Noroozi et al., 2018). In Europe, forests cover 41% of the total mountain area with the majority of forest cover occurring in the Alps, Carpathians and Pyrenees Mountains (Price et al., 2011). Unfortunately, mountain forests are among the most sensitive ecosystems to climate change, with high mountain environments experiencing more rapid changes in temperature than low-elevation environments (Pepin et al., 2015). Since 2001, all major European alpine systems have witnessed an increasing trend in warm-adapted species (Gottfried et al., 2012), illustrating their sensitivity to warmer temperatures. Given that climate influences significantly the structure, composition and function of high mountain ecosystems (Prentice et al., 1992), climate-induced changes are likely going to be more pronounced near the upper treeline (Harsch et al., 2009).

Norway spruce (*Picea abies*) is one of the most important economic trees in Europe, dominating the boreal forests in northern Europe and upper-montane/subalpine areas of the Alps and Carpathian Mountains (hereafter referred to as Carpathians) (Caudullo et al., 2016). Norway spruce is susceptible to both heat and drought due to its shallow root systems and may be vulnerable to the increasing temperatures at high-elevations. In fact, *Picea abies* is currently listed as one of the most vulnerable tree species in the Carpathians due to increasing summer temperatures (Linder et al., 2008), with both montane (1100–1500 m a.s.l) and subalpine (>1500 m a.s.l.) *Picea abies* forests projected to decline in extent with climate change (Werners et al., 2014). Mean summer temperatures in the Carpathians have increased by as much as 2 ^{o}C over the past few decades (Alberton et al., 2017), twice the global mean (Auer et al., 2007), which raises the prospect of greater sensitivity to climate change than montane forests elsewhere in Europe (UNEP, 2007). This sensitivity to climate change will likely propagate through the 21st

91 century, with mean summer temperatures projected to increase by a further 1–2 ^{o}C across the
92 Carpathians by the end of the century (Anders et al., 2014) in conjunction with heat waves and
93 droughts. Projected changes in precipitation across the Carpathians are more varied but suggest
94 greater seasonality with generally drier summers (Anders et al., 2014). If conditions continue as
95 projected, drier conditions could lead to either a collapse and/or dieback of *Picea abies*,
96 compromising the provision of ecosystem services (Lévesque et al., 2013).
97 Many mountains forests including old growth *Picea abies* forests are declining and/or
98 vanishing, especially within the Romanian arc of the Carpathians as a result of deforestation,
99 poor management practices, and increased rates of forest disturbances linked to windthrow, bark
100 beetle outbreak and fire events (Achard et al., 2009; Hlásny and Sitková, 2010; Feurdean et al.,
101 2011; Knorn et al., 2012; 2013; Temperli et al. 2013; Grindean et al., 2019). These factors
102 illustrate the sensitivity of *Picea abies* forests to human intervention, disturbance regimes, and
103 climate change. Given that there is a high likelihood of increased fire risk among central and
104 southern European ecosystems by the end of the 21st century (Lung et al., 2013), and that air
105 temperature is a key variable for establishment and growth of high mountain forests (Körner and
106 Paulsen, 2004), the coupled threat of future climate change and increased likelihood of fires
107 potentially threatens upper-montane *Picea abies* forests across the Carpathians. This threat could
108 affect their ability to provide ecosystem services (Albrich et al., 2018), including negative
109 impacts on key transboundary biosphere reserves (UNESCO-WNBR). However, there is
110 currently a limited understanding regarding the long-term importance of fire in high mountain
111 forests, specifically upper-montane *Picea abies*-dominated forests. This information is critical
112 for conservation and management as *Picea abies* is also highly susceptible to other forest
113 disturbances such as windthrow and bark beetle outbreaks. What limited understanding we have

about fire activity in upper-montane forests throughout the Carpathians is from research mostly from the Eastern and Southern Carpathians, which demonstrate the importance of long-term fire occurrence these elevations (Geantă et al., 2014; Feurdean et al., 2012; 2017; Finsinger et al., 2018; Florescu et al., 2018). No long-term records of fire dynamics existed from the Western Carpathians until recent research, which is from the lower montane forest zone dominated by beech (*Fagus sylvatica*), silver fir (*Abies alba*), and an admixture of Norway spruce (Kołaczek et al., 2020).

Here, we present a new *c.*9500-year high-resolution paleoecological record from Popradské pleso located in the upper-montane forest zone in the High Tatra Mountains, Slovakia, Western Carpathians. We address the existing knowledge gap concerning the long-term history of fire in upper-montane forests in the Western Carpathians by comparing the new record with other high-resolution fire records from the upper-montane forest zone spanning the entire Carpathian region. Our objectives are to; 1) quantify the long-term variability in wildfire (biomass burning) regime and assess spatial differences across the wider Carpathian upper-montane forested ecosystem; 2) evaluate the respective roles of climate and humans as drivers of past biomass burning; 3) explore how forest composition and density modulates biomass burning in these upper-montane forest ecosystems; and 4) use the paleofire record to infer the potential impacts of future climate warming (1–2 ^{o}C). Our study provides critical data for understanding the role of fire disturbance regimes in old growth spruce forests in the Carpathians, with utility for understanding the future dynamics of equivalent montane ecosystems elsewhere.

2 Study region

2.1. Popradské pleso in the Western Carpathians

Popradské pleso (pleso is Slovak for 'glacial lake') (49°09′13" N, 20°04′47" E, 1513 m a.s.l.) is located in the Mengusovská dolina valley, on the south slope of the central High Tatra Mountains (Figure 1). The High Tatra Mountains are a west-to-east trending mountain range along the Slovakia-Poland border situated within the Western Carpathians. This mountain range was heavily glaciated during the Last Glacial Maximum with the Mengusovská dolina valley hosting the largest glacier on the south slope (Zasadni and Kłapyta, 2014). Popradské pleso has a large catchment to lake area ratio (67.5:1), and a maximum water depth of ~18 m with a surface area of ~6.3–6.9 ha (Schaffer and Stummer, 1933; Pacl, 1973). The lake catchment has a granite-granodiorite bedrock and is surrounded by the tallest mountain peaks in the entire High Tatra region including the tallest mountain peak, Rysy (2500 m a.s.l.). The lake has one inflowing stream, Ľadový potok, on the northeast side, and one outflow stream, Krupá, on the south side.

Popradské pleso is located ~50 m downhill from the upper treeline in the upper-montane forest belt (Grodzińska et al., 2004), which is dominated by Norway spruce with an admixture of Swiss stone pine (*Pinus cembra*) and dwarf mountain pine (*Pinus mugo*). While beech (*Fagus sylvatica*) and Silver fir (*Abies alba*) are both common at these elevations in the Southern Carpathians, *F. sylvatica* is currently absent and *A. alba* is very rare at these elevations in the High Tatras (Rybníčková and Rybníček, 2006). However, *F. sylvatica* is present at lower elevations near Štrbské Pleso (1358 m; see Kučera, 2012 and Flachbart, 2007).

Climate in the high Western Carpathian mountain zone is cold and moist, with the highest quantities of precipitation (2000 to 2400 mm yr^{-1}) in the Carpathians occurring in the High Tatra Mountains (UNEP, 2007). Mean annual temperature and precipitation from the closest meteorological station to Popradské pleso, Štrbské Pleso, are 3.7 °C and 1826 mm (Slovak Hydrometeorological Institute), respectively. The local west-to-east mountain

orientation has resulted in a strong windward/leeward precipitation gradient with the north side receiving more precipitation than the south site (Koncek, 1974). Mean annual temperatures range between 2 to -4 ºC in the coniferous belt dominated by *Picea abies* forests (Hess, 1965; 1974). For the High Tatras, climate models suggest 2 ºC warming alongside 5–8% decreases in summer precipitation, with ~10–15% increases in winter precipitation by the end of 21st century (Anders et al., 2014).

2.2. Eastern and Southern Carpathian study sites

Poiana Ştiol (47º35'14" N; 24º48'43" E, 1540 m a.s.l.; Feurdean et al., 2017) and Tăul Muced (47º34'26" N; 24º32'42" E, 1360 m a.s.l.; Feurdean et al., 2017) are both located in the Rodna National Park and Biosphere Reserve, Eastern Carpathians. Poiana Ştiol is a nutrient-poor fen located at the current treeline ecotone dominated by *Picea abies*, *Pinus mugo*, *P. cembra* and *Juniperus communis* ssp. *nana* (Tanţău et al., 2011; Feurdean et al., 2016). The surrounding forest is composed of ~80% *Picea abies* and ~20% *Abies alba* (Topographic Maps of Romania, 1986). Tăul Muced is an ombrotrophic bog within a closed conifer forest, with onsite woody vegetation consisting of *Picea abies* with *P. mugo*. The surrounding forest is comprised of ~40% *Picea abies* and *Abies alba* and ~10% *Fagus sylvatica* (Topographic Maps of Romania, 1986). The climate at Poiana Ştiol is slightly wetter than at Tăul Muced due to its higher altitude (1300 mm and 1200 mm, respectively). Mean annual temperature is 2–2.2 °C at both sites (Dragotă and Kucsicsa, 2011). For the Southern Carpathians, climate models suggest 2 ºC warming alongside 10–15% decreases in summer precipitation, with ~10–15% increases in winter precipitation by the end of 21st century (Anders et al., 2014).

Lake Brazi (45°23'47" N; 22°54'6" E, 1740 m a.s.l.; Magyari et al., 2012) is a small (~0.4 ha), shallow lake (maximum water depth 1.1 m), located in the Retezat National Park, Retezat Mountains, Southern Carpathians. The site is located about 110 m below the timberline in a mixed conifer forest dominated by *Picea abies* and *Pinus cembra*, with *P. mugo* being restricted to the floating *Sphagnum* bog found along the lakeshore. Annual precipitation ranges between 900 and 1800 mm, while the mean annual temperature is around 6 °C in the foothill zone and -2 °C at 2500 m a.s.l. in the Retezat Mountains (Bogdan, 2008). For the Southern Carpathians, climate models suggest 2 °C warming alongside a 10–15% decrease in summer precipitation and a ~2–5% decrease in winter precipitation by the end of 21st century (Anders et al., 2014).

3 Methods

3.1 Field work

In September 2015, a 28 cm (POP 15-GC1) and a 4 m-long core (POP 15–1, drives 1–4) were extruded using a floating platform from the centre of Popradské pleso (water depth, 11 m). The sediment water interface was collected using a short gravity corer (Boyle, 1995), while a Russian corer was used to collect the long-core sediments in 1.5 m overlapping sections. Sediments were stored under refrigeration until they were subsampled at high-resolution (contiguous 0.5 cm intervals) for dating and geochemical analyses.

3.2 Lead 210 and radiocarbon dating

A total of 12 Accelerator Mass Spectrometry (AMS) radiocarbon (^{14}C) ages and a radiometric ^{210}Pb series were obtained to construct an age-depth model for Popradské pleso

205 (Table 1). Most ^{14}C ages were measured on terrestrial plant macrofossils, but in the section
206 below 1371 cm below the water surface, ages were measured on bulk pollen concentrations
207 because of the lack of macrofossils. Pollen extractions for bulk pollen concentrations were
208 modified after Brown et al. (1989) using a dilute Schulze solution of 10% $KClO_3$ and 35% HNO_3
209 (Gray, 1965).
210 Radiometric dating targeted the upper 8 cm of the gravity core (POP-15-GC1), analysing
211 for ^{210}Pb, ^{226}Ra, ^{137}Cs and ^{241}Am by direct gamma assay in the Liverpool University
212 Environmental Radioactivity Laboratory using Ortec HPGe GWL series well-type coaxial low
213 background intrinsic germanium detectors (Appleby et al. 1986). ^{210}Pb was determined via its
214 gamma emissions at 46.5 keV, and ^{226}Ra by the 295 keV and 352 keV-rays emitted by its
215 daughter radionuclide ^{214}Pb following 3 weeks storage in sealed containers to allow radioactive
216 equilibration. ^{137}Cs and ^{241}Am were measured by their emissions at 662 keV and 59.5 keV
217 respectively. The absolute efficiencies of the detectors were determined using calibrated sources
218 and sediment samples of known activity. Corrections were made for the effect of self-absorption
219 of low energy-rays within the sample (Appleby et al. 1992).
220 Age-depth relationships were modeled in a Bayesian framework using 'BACON'
221 (Blaauw and Christen, 2011), including both the ^{210}Pb and ^{14}C dates. All ^{14}C dates were
222 calibrated using the IntCal13 dataset (Reimer et al., 2013).
223
224 ***3.3 Lithostratigraphy, magnetic susceptibility and geochemical analyses***
225 Prior to subsampling, high resolution digital line-scan photographs of the Pop15-1 core
226 were taken using the University of Liverpool Geotek Multi-sensor core logger (MSCL-XZ).
227 Geochemical data were determined non-destructively on a wet sediment basis at 5 mm resolution

using an Olympus Delta ED-XRF (4 W) mounted to the Geotek. Cores were measured under Soil mode (40 kV, 40 kV (filtered) and 15 kV beam intensities) for heavier elements and MiningPlus mode (40 kV and 15 kV) for lighter elements. Each beam intensity ran for 20 seconds with total runs of 60 seconds (soil mode) and 40 seconds (mining plus). The Olympus XRF instrument is subject to daily consistency checks and regular testing using library of certified geochemical reference materials (Boyle et al., 2015). Element concentrations are expressed in ppm, but are subject to possible matrix effects induced by variable down-core water and organic content arising from measuring wet sediments. Magnetic susceptibility (XLF) was measured on a wet sediment basis at 5 mm intervals using a Bartington Instruments MS2E high resolution point sensor paired to the Bartington MS3 meter mounted on the Liverpool Geotek MSCL-XZ. The scan XLF data reveal changes between minerogenic (positive values) and organic or high-water content sediments (negative or diamagnetic values).

3.4 Plant macrofossils and pollen analysis

Pollen analysis was conducted contiguously at 1 cm resolution throughout the gravity core, and at 2.5 cm resolution throughout the long core from Popradské pleso. Pollen processing utilized standard acid-base rinse procedures (Faegri et al., 1989) using 0.5 cm^3 of sediment per sample. A *Lycopodium* tablet was added to each sample prior-to pollen processing, and was used as an exotic tracer to calculate both pollen concentration (grains cm^3) and pollen accumulation rates (pollen influx; grains cm^{-2} yr^{-1}) (Stockmarr, 1972). A minimum of 500 terrestrial pollen grains were identified at a magnification of 400× with the aid of reference material and identification keys (Beug, 2004; Punt, 1976–1996). Pollen counts were converted into pollen percentages based on the abundance of each pollen type relative to the sum of all identified

terrestrial pollen. The pollen profile was divided into pollen assemblage zones based on optimal splitting by sums-of-squares using the broken-stick model using the software, Psimpoll (Birks and Gordon, 1985; Bennett, 1996). Legacy pollen data from the wider Carpathian region were available from Poiana Ştiol, Tăul Muced and Lake Brazi (see Magyari et al., 2012; Tanţău et al., 2011; Grindean et al., 2019). To access changes in forest density, we calculated an index using the ratio of *Picea abies* pollen (a) to *Pinus* pollen (b) following Higuera et al. (2014).

Plant macrofossil analysis was conducted every 2.5 cm from Popradské pleso using standard procedures described by e.g. Birks (2007). Sediment volume was measured by water displacement in a measuring cylinder (1–5 ml), and then gently sieved through a 100 μm sieve. Plant macrofossils were analysed using a stereomicroscope at a magnification of 15–50×, and were identified with the aid of identification keys (Cappers et al., 2006; Bojňanský and Fargašová, 2007; Katz et al., 1977; Tomlinson, 1985) and the herbarium collection at Charles University.

3.5 Charcoal analysis, fire-event detection, and change point analysis

Macroscopic charcoal was analysed at 1 cm resolution in both the gravity core and long core from Popradské pleso. Sediment sub-samples of 1 ml were left for 12 hours in 10 ml, 5% solution of potassium hydroxide (KOH), to disaggregate organic matter. In order to bleach non-charred material, 5 ml of sodium hypochlorite (10% NaOCl) was added to the samples. The required length of bleaching process was adjusted according to the results of test specimens taken from the same sediment core. Samples were screened using a 125 μm sieve and washed into petri dishes. The majority of the non-charred organic particles were manually removed using a stereomicroscope before capturing images of charcoal fragments using a custom-built scanning

device (www.microspock.cz). Images were analysed using ImageJ to count and measure the area of charcoal particles (Schneider et al., 2012). Macroscopic charcoal counts were transformed to concentrations (particles/area cm^{-3}) and accumulation rates ($CHAR_C$ (the number of particles cm^{-2} yr^{-1}).

The site-specific fire history was determined using the CharAnalysis software (Higuera et al., 2009). First, the $CHAR_C$ record was interpolated to a constant temporal resolution of 30 years, which is based on the median sediment accumulation rate. Then, the charcoal record was decomposed into a background component ($CHAR_{back}$), and a peak component ($CHAR_{peak}$), which represents either a single fire event or several temporally clustered fire events within the charcoal-source area. $CHAR_{back}$ was calculated using a moving median smoothed with a 400-year moving-window that ensured a sufficient signal-to-noise index (SNI >3) (Kelly et al., 2011). The residual series ($CHAR_{peak}$) was obtained by subtracting $CHAR_{back}$ from $CHAR_C$, as we assume additive processes are responsible for increased charcoal delivery to the sedimentary basin. Fire episodes were inferred from $CHAR_{peak}$ by fitting a Gaussian mixture model to each overlapping 400-year window while assuming two sub-populations: $CHAR_{noise}$ and fire. This enables modelling both the mean and variance of the $CHAR_{noise}$ distribution locally. The $CHAR_{peak}$ exceeding the 99^{th} percentile of the modeled $CHAR_{noise}$ distribution were considered peak events. Each peak that exceeded the locally defined threshold was statistically screened using the minimum-count test ($p<0.05$) (Higuera et al., 2010).

Change point analysis was used to determine significant changes in biomass burning (i.e. fire activity) for all charcoal records based on variations in both the mean and variance of $CHAR_C$ using a penalty (β) = 6 log(n) (Killick and Eckley, 2014). We also tested the potential

296 effect of sedimentation-rate change on change point detection following Finsinger et al. (2018)
297 using the 'change point' v2.2.2 package (Killick and Eckley, 2014).
298
299 ***3.6 Regional biomass burning***
300 To disentangle local and regional drivers of fire in upper-montane forests in the
301 Carpathians, the use of multiple sites, elevations and quantitative inter-site comparisons are
302 necessary (Gavin et al., 2006). To reconstruct regional variations in biomass burning over time,
303 we compared the record from Popradské pleso to three previously analysed sedimentary charcoal
304 profiles from Poiana Ştiol, Tăul Muced and Lake Brazi (Figure 1). These three sites were chosen
305 based on the following criteria; 1) all sites are currently located in *Picea abies*-dominated forests
306 at/near treeline; 2) all records are temporally well-constrained with limited hiatuses (see
307 Feurdean et al., 2015; 2016; Finsinger et al., 2014); and 3) pollen and high-resolution charcoal
308 data are available from each site, and span the majority of the Holocene. All fire histories were
309 determined using the CharAnalysis software (Higuera et al., 2009) and followed the same
310 methodologies presented in section 3.6 to allow for regional comparisons of biomass burning
311 histories.
312
313 ***3.7 Local climate model***
314 To reconstruct the influence of broad-scale changes in climate on fire activity at
315 Popradské pleso, we developed a locally-derived macrophysical climate model (MCM; Bryson,
316 2005) using meteorological data of the Slovak Hydrometeorological Institute from the closest
317 weather station, Štrbské pleso. For more information about the MCM, please see Carter et al.
318 (2018).

3.8 Generalized Additive Models

Generalized additive models (GAMs; Hastie and Tibshirani, 1986) use a link function to investigate the relationship between the mean of the response variable (i.e. dependent variable) and a smoothed function of the predictor variable (i.e. independent variable). In this study, we investigated the relationship between biomass burning (e.g. total $CHAR_C$ from each of the four study sites) and *Picea abies*, *Pinus*, primary forest cover (i.e., the summed percentage values of *Picea abies* and *Pinus*), forest density (the ratio of *Picea:Pinus*), and human indicators. Given that many secondary human indicator taxa were naturally abundant in the early Holocene (Fyfe et al., 2015), we used a base period from 8000 cal yr BP to present in the model to remove any bias secondary indicator pollen taxa may have in the early Holocene before the intensification of human activity (see SI Table 1 for complete list of indicator taxa). We used a quasi-Poisson distribution with a log link function using the 'mgcv' package (Wood, 2017) in R. The GAMs were fit using restricted maximum likelihood smoothness selection.

4. Results

4.1 Popradské pleso chronology

The gravity core (POP-15-GC1) shows a very low accumulation rate with $^{210}Pb/^{226}Ra$ equilibrium at a depth of around 7 cm (Figure 2). The exponential decline in unsupported ^{210}Pb concentrations with depth suggests a relatively uniform sedimentation rate throughout the period of time spanned by the ^{210}Pb record. High ^{137}Cs concentrations in the uppermost 2 cm most probably record fallout from the 1986 Chernobyl accident. Although the ^{137}Cs record from nuclear weapons test fallout again appears to have been obscured by Chernobyl ^{137}Cs, the 1963

342 fallout maximum is recorded by the presence of significant concentrations of ^{241}Am between 2–4
343 cm. ^{210}Pb ages calculated using the CRS and CIC models (Appleby and Oldfield 1978) both
344 suggest a relatively uniform sedimentation rate since the middle of the 19th century with a mean
345 value during that time of 0.0065 ± 0.0008 g cm^{-2} y^{-1} (0.048 cm y^{-1}). These results place 1986 at a
346 depth of between 1–2 cm and 1963 between 2–3 cm, in reasonable agreement with the depths
347 suggested by the ^{137}Cs and ^{241}Am records. The base of the ^{210}Pb age-depth model is consistent
348 with European increases in airfall stable Pb concentrations in the sediment, associated with
349 industrialization from the 1850's onwards (Renberg et al., 2000).
350 Previous research from Popradské pleso suggested the possibility of a hiatus at the
351 transition between the Late Glacial and the Holocene (Rybníčková and Rybníček, 2006). We
352 found an age difference of ca. 4000 ^{14}C years between depths 1374.5 cm and 1371 cm below the
353 water surface (Table 1). As core lithology changes dramatically at depth 1371.5 cm, transitioning
354 from inorganic glacial sediments into organic-rich gyttja (Figure 3), we confirm the
355 sedimentation hiatus originally suggested by Rybníčková and Rybníček (2006). Due to multiple
356 age-reversals between the bottom of the core (depth 1635 cm) and depth 1373 cm, the age-depth
357 model and the basal age for Popradské pleso are insufficiently constrained. Therefore, we will
358 only present and discuss the section of the sedimentary profile reflecting continuous
359 accumulation spanning the Holocene (Figure 3).
360
361 ***4.2 Reconstructed vegetation dynamics at Popradské pleso***
362 Summarising the dominant canopy taxa and significant changes in understory at
363 Popradské pleso, the pollen percentage profile was divided by six statistically significant pollen
364 assemblage zones (SI Figure 1). Zone 1 (age undetermined; depth 1380–1370 cm) probably

captures the Younger Dryas/Holocene transition, but due to a hiatus we were unable to confirm the exact ages of this zone. Regardless, this zone is characterized by high percentages of *Pinus* (>50%) and non-arboreal pollen (NAP; >20%), and by low percentages of *Picea abies* (<10%) similar to that found by Rybníčková and Rybníček (2006) (SI Figure 2). Low percentages of low-elevation arboreal species such as *Corylus avellana* were also recorded in this zone (SI Figure 1). No plant macrofossils were found in Zone 1. Zone 2 (9500–8500 cal yr BP; depth 1370–1355 cm) is characterized by an increase in *Picea abies* percentages (~15%), with relatively high values of *Picea abies* influx values (~1000 grains cm^{-2} yr^{-1}), the presence of *Picea abies* stomata, and high concentration of *Picea abies* macrofossils. *Pinus* percentages (~20%) and influx (>2000 grains cm^{-2} yr^{-1}) values both declined from the previous zone, however *Pinus* stomata and macrofossils, both *Pinus* sp. and *P. cembra* are present throughout this zone (Figure 4). While total herbaceous percentages decreased to their lowest values, several herbaceous macrofossils were found in Zone 2, such as an *Alchemilla* sp. seed, a *Caltha palustris/Trollius altissimus* seed, and a Poaceae seed (SI Figure 1). *Larix* pollen was not found in Zone 2, however, *Larix decidua* needles were found. Zone 3 (8500–5600 cal yr BP; depth 1355–1293 cm) can be characterized by the local dominance of *Picea abies* and *Pinus* with pollen percentages averaging 15–20%, and pollen influxes averages 2823 grains cm^{-2} yr^{-1} and 3335 grains cm^{-2} yr^{-1}. *P. cembra* needles decreased during this zone, while *Pinus.* sp (most likely *P. mugo*) needles and bud scales increased. *Corylus avellana* percentages and influxes continued to decrease in this zone. High abundances of macrofossils were found at the onset of Zone 3; for example, seeds from *Rubus idaeus*, *Alchemilla* sp. and *Juncus* sp. and *Rumex acetosa* fruit. Zone 4 (5600–3900 cal yr BP; depth 1293–1248 cm) is notable in that both *Abies alba* and *Fagus sylvatica* pollen percentages and influxes slowly increase during this zone (SI Figure 1). *Picea*

388 *abies* pollen percentages and influxes also increase to their highest values (~37% and ~7400
389 grains cm^{-2} yr^{-1}) of the entire Holocene record before beginning a long-term declining trend.
390 Zone 5 (3900–800 cal yr BP; depth 1248–1133 cm) is characterized by a decreasing trend in both
391 *Picea abies* pollen percentages and influxes, despite the high abundances of *P. abies* needles
392 being recorded. *Pinus* pollen percentage values (~20%) were relatively stable, with high
393 abundances of *P. cembra* needles being recorded in Zone 5. *Abies alba* and *Fagus sylvatica*
394 reached their highest percentages (15% and 11%) and influx values (~1900 grains cm^{-2} yr^{-1} and
395 1160 grains cm^{-2} yr^{-1}), and human impact indicator pollen percentages and influxes begin to
396 increase during this zone. *Sphagnum* sp. capsules were also prominent in this zone. The final
397 zone, Zone 6 (800 cal yr BP– present; depth 1133–1100 cm) is characterized by declining
398 percentages of trees and shrubs, specifically *Picea abies*, *Fagus sylvatica*, and *Abies alba*.
399 However, pollen influx for each of these species shows rapid variability instead of a declining
400 trend. Pollen percentages and influx values of *Pinus* and of human indicators increase throughout
401 Zone 6. Macrofossils were not analysed from Zone 6.
402
403 ***4.3 Reconstructed fire and erosion history at Popradské pleso***
404 Elevated $CHAR_C$ values were recorded between 9000 and 7000 cal yr BP, with low
405 values between 5500 and 1000 cal yr BP and then elevated values again in the last ~1000 years
406 (Figure 4). The change-point analysis shows three periods of high biomass burning; 9000-7000
407 cal yr BP, around 6800 cal yr BP, and the past 2000 years (Figure 4). A total of 24 fire episodes
408 were detected over the past 9500 years, with periods of increased fire frequency centred between
409 9000–8500 cal yr BP, 7000–6000 cal yr BP, and over the last 3000 years. During the past 200
410 years, one single event was identified in the $CHAR_C$ record (see black circle, Figure 4).

411 However, based on documentary evidence, this is a false positive because no fire event has
412 occurred at Popradské pleso over the last 200 years. The increase in $CHAR_C$ is possibly due to
413 the charcoal being produced from the Horský Hotel Popradské Pleso which was built on the
414 shore of Popradské pleso in the mid-1800s. Fire frequency averages ~2.5 fires/1000 years (or a
415 fire return interval of ~400 years) throughout the entire record.
416 XRF geochemical profiles for K, Ti, Rb and Zr (Boyle, 2011; Davies et al., 2015),
417 alongside magnetic susceptibility (XLF) data (Dearing 1992; Oldfield et al., 2003), show
418 changes in the flux of lithogenic elements from the granitic bedrock catchment. The inorganic
419 stratigraphy (Figure 4) displays two types of behavior, 1) sharp and short-lived peaks and 2)
420 changes in the background concentrations of these lithogenic markers. Ratios for the typically
421 insoluble lithogenic elements, Zr and Rb, provide additional information on sediment grain size,
422 with Zr typically coarse silt whereas Rb, Ti and K associate with finer fractions (Boyle, 2001;
423 Davies et al., 2015). The peaks in lithogenic elements occur throughout the Holocene, but are
424 larger in magnitude 8500-7750, 6500-5500 and >4500 cal yr BP. Coincidentally, these periods
425 align with periods of increased biomass burning as detected by change point analysis. These
426 peaks across all lithogenic elements reflect short-lived run-off extreme events (e.g. storms or
427 rapid snowmelt), with coincident peaks in Zr/Rb reflecting the higher-energy riverine delivery of
428 coarser sediments to the lake. For many layers, particularly >4500 cal. yr BP, the Zr/Rb peak
429 often occurs early in the erosion event before finer grain size show declining energy in the event.
430 The background quantities for these lithogenic markers and the associated general erosion
431 regime also changes, with lower concentrations for the earlier Holocene, but increasing in both
432 their concentration and grain size (Zr/Rb) after 4500 cal yr BP.
433

4.4 Modeling biomass burning-vegetation relationships across the Carpathians

At Lake Brazi, biomass burning significantly increases with increasing *Pinus* and *Picea abies* abundance ($p<0.001$) and increasing primary forest cover ($p<0.001$), and significantly decreases with forest density ($p<0.001$) (Table 2). Human indicators have a negligible effect on biomass burning at Lake Brazi ($p=0.682$) (Figure 7). At Poiana Ştiol, biomass burning significantly increases with increasing forest density ($p<0.001$) and primary forest cover ($p<0.03$). Both *Pinus* ($p=0.319$) and *Picea abies* ($p=0.45$) abundance and human indicators ($p=0.104$) all had insignificant effects on biomass burning. At Popradské pleso, *Pinus* and human indicators were both found to positively ($p<0.001$) influence biomass burning. Biomass burning decreased with increasing *Picea abies* ($p<0.001$) and increasing forest density ($p<0.001$) at Popradské pleso. Primary forest cover had a negligible effect on biomass burning at Popradské pleso ($p=0.298$). Finally, at Tăul Muced, biomass burning significantly increases with increasing primary forest cover ($p<0.002$) and *Picea abies* ($p<0.003$) pollen. Forest density ($p=0.369$), human indicators ($p=0.389$), and *Pinus* pollen ($p=0.624$) all had insignificant effects on biomass burning.

5 Discussion

The new data on biomass burning ($CHAR_C$) from the High Tatra Mountains follows similar burning patterns to those experienced at the other upper-montane Carpathian sites during the Holocene (Figure 5). Both in the High Tatras as well as at other Carpathian sites, forests were dominated by *Picea abies,* a fire avoider species with minimal fire adaptations (Feurdean et al., 2017), and often associated with reduced fire activity (Ohlson et al., 2011). As a consequence,

456 minimal biomass burning would be expected, yet biomass burning has been an agent of forest
457 disturbance prevalent in the Carpathians through the Holocene.
458
459 ***5.1 Holocene wildfire activity across the Carpathians***
460 ***5.1.1 Early and mid-Holocene***
461 In the upper-montane forest zone, higher rates of biomass burning (i.e. total $CHAR_C$)
462 were recorded between 10,000–6000 cal yr BP at Popradské pleso, Lake Brazi and Poiana Ştiol,
463 as indicated by both change point analysis and increased fire frequencies (Figure 5). Higher
464 $CHAR_C$ is likely connected to broad-scale climate, with summer temperatures significantly
465 warmer-than-present as a result of peak summer insolation (Berger and Loutre, 1991). Increased
466 abundances of *Pinus cembra* and *P. mugo* macrofossils at Lake Brazi, (Finsinger et al., 2018), *P.*
467 *cembra* and *Pinus* sp. (likely either *P. cembra* or *P. mugo*) macrofossils at Popradské pleso
468 (Figure 4), and *P. sylvestris/mugo* macrofossils at Poiana Ştiol (Feurdean et al., 2016) were
469 found during the early and mid-Holocene suggesting a more open upper-montane landscape,
470 which is supported by lower *Picea:Pinus* ratio values until ~8500 cal yr BP (Figure 6). Warmer
471 conditions in the early Holocene, coupled with generally higher abundances of *Pinus* sp. likely
472 *P. mugo* or *P. cembra*, created a positive climate-fuel relationship that resulted in higher amounts
473 of biomass burning. We acknowledge *P. sylvestris* may have potentially been present in the early
474 Holocene, as its pollen is indistinguishable from *P. mugo*. However, given that each study site is
475 currently surrounded by either *P. mugo* or *P. cembra*, we hypothesize these two species were
476 influencing biomass burning in the early Holocene. Long-term paleoecological records indicate
477 that the late-successional *P. cembra* is able to withstand moderately frequent surface fires, but
478 not high anthropogenic fire activity (Ali et al., 2005; Genries et al., 2009; Blarquez and

479 Carcaillet, 2010; Schwörer et al., 2015), while the woody shrub, *P. mugo*, is favored by fire
480 disturbances under drier conditions (Stähli et al., 2006; Leys et al., 2014). Modeled *Pinus*
481 response curves demonstrate a significant relationship with biomass burning at Lake Brazi and
482 Popradské pleso (Table 2). This suggests that forest composition with higher amounts of *P. mugo*
483 and/or *P. cembra*, despite the prevalence of *Picea abies*, may have been especially important for
484 influencing biomass burning, especially at Lake Brazi and Popradské pleso.
485 High biomass burning during the early and mid-Holocene is witnessed across Europe
486 (Marlon et al., 2013; Feurdean et al., 2012; 2013; 2017; Clear et al., 2014; Vannière et al., 2016;
487 Dietze et al., 2018; Florescu et al., 2019), as well as throughout the Western Carpathian region.
488 For example, in the Polish Western Carpathians, biomass burning was highest between 10,000–
489 9500 cal yr BP and 7500–6000 cal yr BP at lower-montane forests (Kołaczek et al., 2020). At
490 Belianske lúky, Slovakia's largest spring fen located near the foothills of the High Tatra
491 Mountains approximately 30 km from Popradské pleso, high macrocharcoal abundances were
492 recorded ~8500 cal yr BP as a result of drier conditions (Hájková et al., 2012). These results
493 from Belianske lúky generally agree with high $CHAR_C$ values at Popradské pleso. However, at
494 Popradské pleso, both $CHAR_C$ and fire frequency decrease and remaine low, while indicators for
495 soil erosions (i.e. K, Ti, Rb and XLF) all increase between 8400 and 7000 cal yr BP (Figure 3).
496 Interestingly, this time period overlaps with a potential sediment hiatus in the Polish Carpathian
497 Mountains as a result of wetter conditions which caused the loss of sediment deposits (Kołaczek
498 et al., 2020). Increased erosion is also recorded in both the Beskid Makowski Mountains and
499 Beskid Wyspowy Mountains during this same time period (Margielewski, 2006; 2018). The time
500 period between 8400 and 7000 cal yr BP overlaps with a period of global rapid climate changes
501 (Mayweski et al., 2004), that is well documented across the entire Carpathian region, either by an

increase in moisture (Hájková et al., 2016; Jamrichová et al., 2018; Šolcová et al., 2018; Dabkowski et al., 2019), reoccurring fire events (Pál et al., 2016; 2018; Vincze et al., 2017; Florescu et al., 2019), or as a change in climatic conditions or erosion activity (Schnitchen et al., 2006; Feurdean et al., 2008; Tóth et al., 2015; Gałka et al., 2020). Together, this data suggests climate as the ultimate driver of biomass burning in the Carpathians in the early and mid-Holocene.

However, archaeological evidence demonstrates human occupation and activity near the High Tatra Mountains and throughout the Carpathian Basin since at least the Mesolithic period ~10,000 cal yr BP (Valde-Nowak and Soják, 2010; Kertész, 2002 and references therein). Florescu et al. (2018) found an increase in biomass burning ~8500 cal yr BP in the Southern Carpathians which coincided with a slight increase in meadow and pasture pollen types, suggesting that Early-Middle Neolithic (~8000 cal yr BP) populations occupied montane forest-elevations in the Southern Carpathians. Both Cerealia and *Secale* were first identified at Tăul Muced ~7300 cal yr BP (Feurdean et al., 2017) illustrating a long history of human occupation in the Southern Carpathians. Similarly, others have also documented, or hinted at the possible presence of humans at montane-elevations in the Southern Carpathians in the late Neolithic (Fărcaş et al., 2003; 2013; Feurdean et al., 2016; 2017). However, because certain taxa typically classified as secondary human indicator species (e.g. *Rumex*, Poaceae, *Plantago*) are apophytes and were naturally and abundantly present during the early Holocene, these data were left out of the GAMS model prior to 8000 cal yr BP, and thus our results are only indicative of anthropogenic activity post 8000 cal yr BP. It may be that Mesolithic and Neolithic populations were foraging seasonally among the Carpathians both in the lowlands and at higher-elevations, however, palynological evidence does not illustrate large-scale changes in vegetation at any of

525 the study sites (Figure 5). While low density Mesolithic/Neolithic populations could have
526 contributed to the overall rate of biomass burning in the early and mid-Holocene, we suggest
527 climate was the ultimate driver of early and mid-Holocene burning in upper-montane forests.
528
529 ***5.1.2 Mid to late Holocene***
530 Biomass burning was reduced in the regions' upper-montane forest zone from ~6000 to
531 ~2000 cal yr BP (Figure 5) as a result of cooler and wetter conditions. Cooler and wetter
532 conditions led to denser *Picea abies* upper-montane forests (Figure 6), which naturally
533 modulated biomass burning by regulating understory microclimates (Chen et al., 1999; Davis et
534 al., 2018). Thus, this coupled climate-fuel relationship led to an overall reduction in biomass
535 burning in upper-montane forests across the Carpathians (Feurdean et al., 2020). However,
536 despite the dominance of *Picea abies*, fires were not excluded from this forest type, which is
537 illustrated by relatively moderate fire frequencies (~2 fires/1000 years) at most sites (Figure 5).
538 At Popradské pleso, a substantial change in the erosion regime occurred ~4000 cal. yr
539 BP, with the gradual increase in the baseline concentrations for lithogenic markers (Zr, K, Ti, Rb
540 and XLF) showing a persistent shift to greater erosion (Figure 4). Increased frequency of coarser
541 and mineral rich layers from ~4000 cal. yr BP suggest also an intensification of the run-off
542 events (e.g. storms or rapid snowmelt) (Schillereff et al., 2014; 2019; Chiverrell et al., 2020).
543 Together, the long-term baseline concentrations and events (i.e. peaks) shown in the erosion
544 proxies both point to increases in moisture and mineral in-wash. Soil erosion processes are
545 highly dependent upon the magnitude of rainfall events (Schumacher at al., 2016), which the
546 MCM model demonstrates is highly variable over the last 4000 years at Popradské pleso (Figure
547 4; summer precipitation curve). We therefore hypothesize that an increase in summer

precipitation could have potentially caused the overall decrease in biomass burning in the Western Carpathians. Our interpretation of an increase in moisture across the region is supported by rising groundwater levels leading to forestless bogs between 4395–4224 and again at 3940–3050 cal yr BP in the Polish Carpathians (Krąpiec et al., 2016), an increase in illuvial deposits in the Beskid Makowski and Beskid Wyspowy Mountains (Margielwski, 2006; 2018; Starkel et al., 2013), as well as a sediment hiatus in the Polish Western Carpathians between 4940–3550 cal yr BP (Kołaczek et al., 2020). The timing of this sediment hiatus in the Polish Western Carpathians is interesting in that it aligns perfectly with a significant reduction in fire frequency at Popradské pleso, thus supporting a climatically driven, regional-scale moisture event. However, this moisture event was not confined to the Western Carpathians. Increased fluvial activity and/or increased moisture was also recorded in the Dniester River valley, Eastern Carpathians (Kołaczek et al., 2018) and in the Rodna Mountains, Eastern Carpathians (Gałka et al., 2016; 2020; Diaconu et al., 2017).

Despite cooler and wetter conditions documented in the late Holocene, the forest density index (i.e. the *Picea:Pinus* ratio) shows a transition from a dense *Picea*-dominated to a more open *Pinus*-abundant system beginning ~3500 cal yr BP at Popradské pleso. This transition is supported by higher abundances of *Pinus cembra* macrofossils ~4000 cal yr BP. A more open landscape may have contributed to the intensification of the run-off events already discussed. However, *P. cembra* and *P. mugo* both have extension root systems that help prevent soil erosion in alpine environments. Thus, the intensification of human activities in the High Tatra Mountain area may have significantly contributed to changes in the forest composition and in biomass burning. The first indication of intense human impact in the High Tatra Mountains is dated to ~4000 cal yr BP (Obidowicz, 1996), which aligns with the first recording of primary human

571 indicator pollen types at Popradské pleso (SI Figure 1). The modeled response curves for
572 Popradské pleso demonstrate a significant positive relationship with biomass burning and human
573 indicator species (Figure 7). Together, this data suggests that intensified human activities at high
574 elevation areas may have contributed to the change in forest density. However, while there is no
575 large-scale change in $CHAR_C$ at Popradské pleso, fire frequency increases at this time (Figure 5),
576 suggesting that humans may have been utilizing small-scale fires to alter upper-montane forest
577 composition as early as ~3500 cal yr BP.

578 Regionally, Cerealia pollen is first recorded ~4400 cal yr BP in the Polish Western
579 Carpathians (Czerwiński et al., 2019), while both Cerealia and *Secale* are present in subalpine
580 sediments ~4200 cal yr BP in the Rodna Mountains, Eastern Carpathians (Geantă et al., 2014).
581 Similarly, Cerealia pollen has been consistently present in the Beskid Wyspowy Mountains,
582 Polish Western Mountains since 2880 cal yr BP along with an increase in fire activity illustrating
583 the connection between land use and fire (Czerwiński et al., 2019). An increase in biomass
584 burning during the Middle (~2600 cal yr BP) and Late Bronze Age (~2100 cal yr BP) may be
585 connected with the utilization of high elevation areas by humans in the Carpathians (Schumacher
586 et al., 2016; Vincze et al., 2017), similar to a well-documented process in the Alps where
587 seasonal pastoralism has resulted in a lowered treeline (Dietre et al., 2016; Tinner, 2007).
588 Feurdean et al. (2020) found that biomass burning increased dramatically in continental regions
589 during the Late Bronze Age and Iron Age as a result of increased deforestation and the creation
590 of arable land. Over the last 2000 years, biomass burning has increased considerably at both
591 Popradské pleso and Tăul Muced. The high rates of biomass burning recorded in the High Tatra
592 Mountains likely reflects regional burning at lower elevations as a result of human activities
593 which is demonstrated by an increase in human indicator species over the last 2000 years (Figure

5), and a concurrent increase in microcharcoal – an indicator of regional biomass burning (SI Figure 1). These data agree with archaeological evidence showing humans first impacted the forests near Belianske lúky ~2000 cal yr BP (Jankovská, 1972). Western Carpathian forests were being affected by intense human activities, specifically through forest clearance by early farmers who used fire as a landscape management tool (Kukulak, 2000; Jawor et al., 2016a, b). Summit grasslands in the nearby Hercynian mid-mountains of central Europe were also affected by human occupation and activity as early as the Iron Age ~1900 cal yr BP (Novák et al., 2010). However, despite regional literature and pollen records discussed here supporting the notion that humans influenced landscapes regionally beginning ~4000 cal yr BP, the modeled response curves illustrate a weak connection between biomass burning and human indicator species at Lake Brazi, Poiana Ştiol and Tăul Muced (Figure 7). This suggests that human activities (i.e. land use) were less extensive in the upper-montane forest zone in Southern and Eastern Carpathians, as previously suggested by Finsinger et al. (2018).

5.2 Forest composition and forest density influences biomass burning in Carpathian upper-montane forests

The interplay between forest composition and forest density significantly influenced the overall patterns in biomass burning found in upper-montane Carpathian forests. Specifically, there is a strong relationship between biomass burning and forest density (i.e., *Picea:Pinus* ratio); when forest density decreases, biomass burning increases (Figures 6 & 7). The forest density index illustrates that biomass burning is highest when landscapes are more open and abundant with *Pinus*, while biomass burning is greatly reduced when dense *Picea abies* forests form (Figure 7). This relationship is also reflected in the modeled primary forest cover (i.e. the

617 sum of *Pinus* and *Picea* pollen) response curves which show that burning increases at
618 intermediate pollen values ranging between ~30–50%. Biomass burning decreases at most sites
619 when primary forest cover is denser (>50% pollen; Figure 7). This suggests that when forests
620 reach a threshold of ~50% primary canopy pollen, forests may be too dense, with an understory
621 either too damp to burn and/or comprising insufficient ground-level fuel to sustain fire spread.
622 While the canopy threshold of ~50% is slightly lower than identified by Feurdean et al. (2020),
623 who suggest biomass burning increases when total forest canopy pollen percentages reaches
624 60%, our results agree with their findings in that biomass burning is reduced when tree cover
625 (deduced from pollen data) reaches certain threshold levels in these upper-montane forests.
626 Together, the modeled response curves illustrate the sensitivity of upper-montane forests
627 to fire through alterations in both forest composition and density. While these results are
628 important for forest management implications, additional research utilizing pollen productivity
629 estimates (PPEs) would be invaluable for forest managers interested in mitigating against future
630 climate change in these forests (see Trondman et al. 2015; Abraham et al., 2016). Although our
631 study is unable to quantify canopy openness due to the lack of adequate sites in the Carpathians
632 used to calculate PPEs, our study does illustrate the need for further fire-related research from
633 the region.
634
635 ***5.3 Future climate change impact on upper-montane Carpathian forests***
636 Future climate projections for the Carpathians forecast an additional 1–2 ºC increase in
637 summer mean temperatures by the end of the 21st century, leading to projected increases in heat
638 waves, droughts and fire activity (Anders et al., 2014; Lung et al., 2013). Both summer and
639 winter precipitation are projected to decrease in the Southern Carpathians, by as much as 10–

640 15% in the summer and 2–5% in the winter (Anders et al., 2014). Whereas in the Western
641 Carpathians, summer precipitation is projected to decrease ~10%, yet winter precipitation is
642 projected to increase by 10% (Anders et al., 2014). These projections suggest that changes in
643 vegetation composition and disturbance regimes may be more pronounced in the Southern
644 Carpathians forests.

645 There is a high confidence that treeline will shift upward in response to warming
646 temperatures (see Greenwood and Jump, 2018 and references therein; Field et al., 2014), which
647 could add additional stress to upper-montane forests already experiencing temperature
648 amplification (Pepin et al., 2015). Our results offer potential analogs with regards to ecosystem
649 responses and the anticipated impact of future climate change and fire risk, hypothetically
650 leading to two different climate-fuel scenarios for these upper-montane forests. First, an upward
651 shift of treeline could result in an increase in *Picea abies*, thereby creating a negative feedback
652 with dense *Picea abies* forests generally suppressing the overall risk of fire. This feedback is
653 generally seen in northern European forests, where a decrease in biomass burning with *Picea*
654 *abies* expansion has been documented (Ohlson et al., 2011). Second, as exemplified by the
655 warmer and drier early to mid-Holocene, *Pinus cembra* and/or *P. mugo* (or potentially *P.*
656 *sylvestris*) could become vulnerable to warming temperatures, thereby developing increased
657 susceptibility to fire danger and constituting a positive climate-fuel feedback. Given that this
658 second scenario resembles more-closely future climate projections for the region i.e. warmer and
659 drier conditions, especially those projected for the Southern Carpathians, we suggest that upper-
660 montane forests may be more vulnerable to fire risk than currently thought, especially upper-
661 montane forests found in the Southern Carpathians.

662 The second scenario has been documented for the wider region. For example, in the Alps,
663 *P. cembra* benefited from above modern mean July temperatures during the mid-Holocene
664 (Colombaroli et al., 2010). Increased drought conditions and reduced precipitation in the mid-
665 Holocene favored *Pinus sylvestris* over *Picea abies*, leading to an increase in fire frequency in
666 the Ural Mountains, Russia (Barhoumi et al., 2019). In the Balkan Bulgarian Mountains, fires
667 mostly occurred in *Pinus*-dominated systems over the last 600 years, however, the largest fire
668 documented historically have recently been in *Picea abies*-dominated forests as a result of
669 humans (Panayotov et al., 2017). Finally, simulations using LandClim from the Alps project an
670 upward shift of vegetation will occur, with *Picea abies* being replaced by *Pinus* in response to
671 higher drought incidence (Schumacher and Bugmann, 2006).
672 Given that our sites from the Carpathians all document a shift to more *Pinus* pollen
673 relative to *Picea abies* at present (Figure 6), and that *Picea abies* forests are projected to decline
674 in extent with climate change (Werners et al., 2014), this second scenario is especially
675 concerning. Our results highlight that biomass burning is a prevalent disturbance agent in upper-
676 montane forests, but these systems may become more vulnerable to an increasing fire risk with
677 climate change. However, other factors such as soil development (Henne et al., 2011) and aspect
678 (Courtney-Mustaphi and Pisaric, 2013) may influence and/or inhibit changes in vegetation
679 composition and disturbance events in these forests in the future. Additionally, intensified land-
680 use practices coupled with increased fire frequency could also influence/inhibit vegetation
681 composition, as witnessed from the Alps (Berthel et al., 2012). Additional research from the
682 region, especially from the Ukrainian Carpathians, that utilize high-resolution, multi-proxy
683 approaches are necessary to fully understand the mechanics and spatial distribution of how
684 upper-montane forests may be impacted with future climate change.

685

686 ***6 Conclusion***

687 Our study provides the first long-term fire record from the upper-montane forest zone
688 from the High Tatra Mountains in the Western Carpathians. Our results demonstrate that fire has
689 been a continuous disturbance agent at Popradské pleso throughout the entire Holocene period.
690 Our results also demonstrate that biomass burning across other upper-montane Carpathian forests
691 is influenced by forest composition and forest density, both of these are strongly-dependent on
692 climate. In the early and mid-Holocene, a positive climate-fuel feedback developed that linked
693 warmer conditions and abundant *Pinus* with higher biomass burning. When climate cooled and
694 became wetter in the late Holocene, climate-fuel relationships created a negative feedback with
695 *Picea abies* modulating less fire activity at upper-montane elevations. However, despite the
696 reduced risk of fire implicit in *Picea abies* forests, biomass burning continued in forests with an
697 intermediate primary forest cover (i.e. 30–50%; sum of *Picea abies* and *Pinus* pollen). These
698 findings suggest that more dense forests (>50% pollen) had microclimate conditions not
699 favorable for fire activity.

700 As temperatures continue to increase across the Carpathian region, so will the rate at
701 which natural disturbances (i.e. windthrow, fire, bark beetle outbreaks) occur, potentially
702 threatening these upper-montane forest ecosystems (see e.g. Seidl et al., 2014). In addition,
703 treeline is expected to migrate upslope in response to increasing temperatures (see Greenwood
704 and Jump, 2018 and references therein), which could alter natural disturbance regimes.
705 Understanding how upper-montane forests and natural disturbance regimes (i.e. biomass
706 burning) may be impacted with future climate change is important as these forests provide many
707 ecosystem services. We hypothesize two potential future scenarios based on our results. First, an

upward migration of treeline could result in an increase in *Picea abies* thereby creating a negative feedback with dense *Picea abies* forests modulating any fire risk. Second, as seen in the early and mid-Holocene when climate was warmer and drier than present, patches of *Pinus cembra* and/or *P. mugo* may potentially become vulnerable to warming temperatures and more susceptible to fire. Our study highlights how forest composition and forest density may influence future fire risk.

Funding

This work was supported by the Czech Science Foundation [EUROPIA project no. 16-06915S], the Ministry of Education-UEFISCDI, Romania (project PN-III-P4-ID-PCE-2016-0711) and by P.G. Appleby and G.T. Piliposian of the Environmental Radioactivity Research Centre at the University of Liverpool who provided the Radiometric (210Pb, 226Ra, 137Cs and 241Am) dating.

Acknowledgement

We would like to thank the High Tatra National Park administration for allowing us to core the Popradské pleso, and Peter Fleischer for his support in the field. We also thank to John Boyle, Ladislav Hamerlík, Fiona Russell, Daniel Schillereff, Jolana Tátosová, and Daniel Vondrák for their assistance during coring.

Main Figures

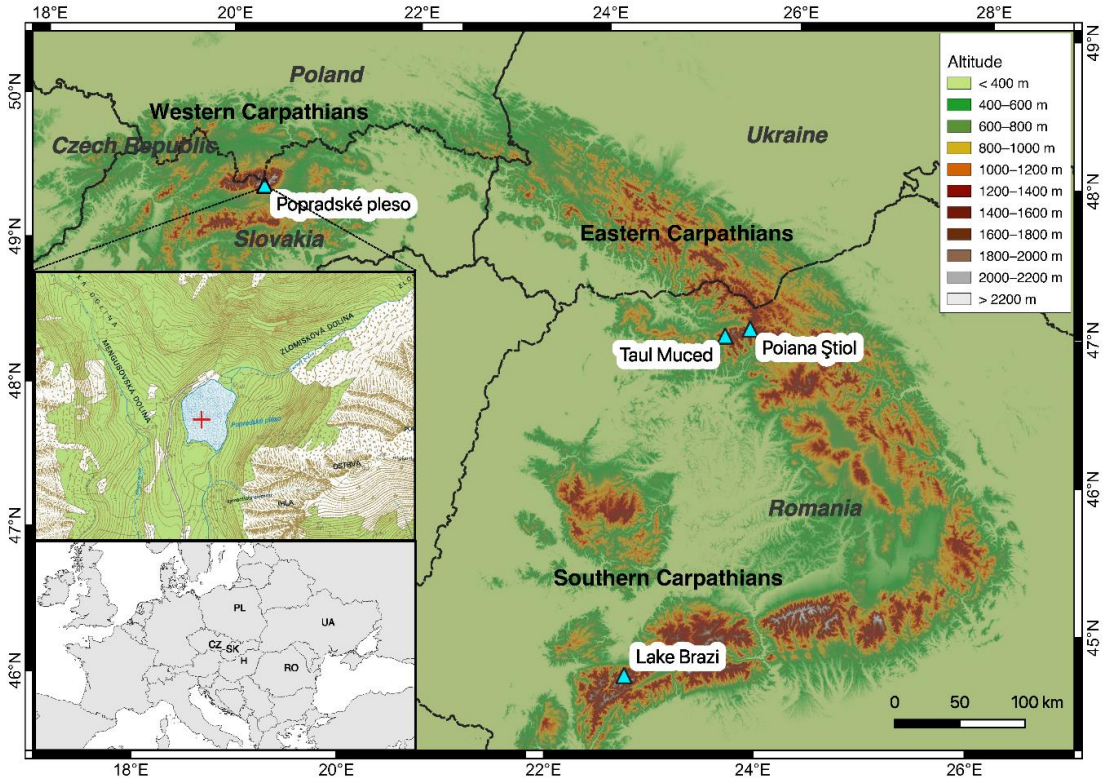

730

731 Figure 1. Map of Popradské pleso, High Tatra Mountains, Slovakia (this study), in relationship to

732 other *Picea abies*-dominated sites discussed; Tăul Muced and Poiana Ştiol, Eastern Carpathians

733 (Feurdean et al., 2017), and Lake Brazi, Southern Carpathians (Magyari et al., 2012).

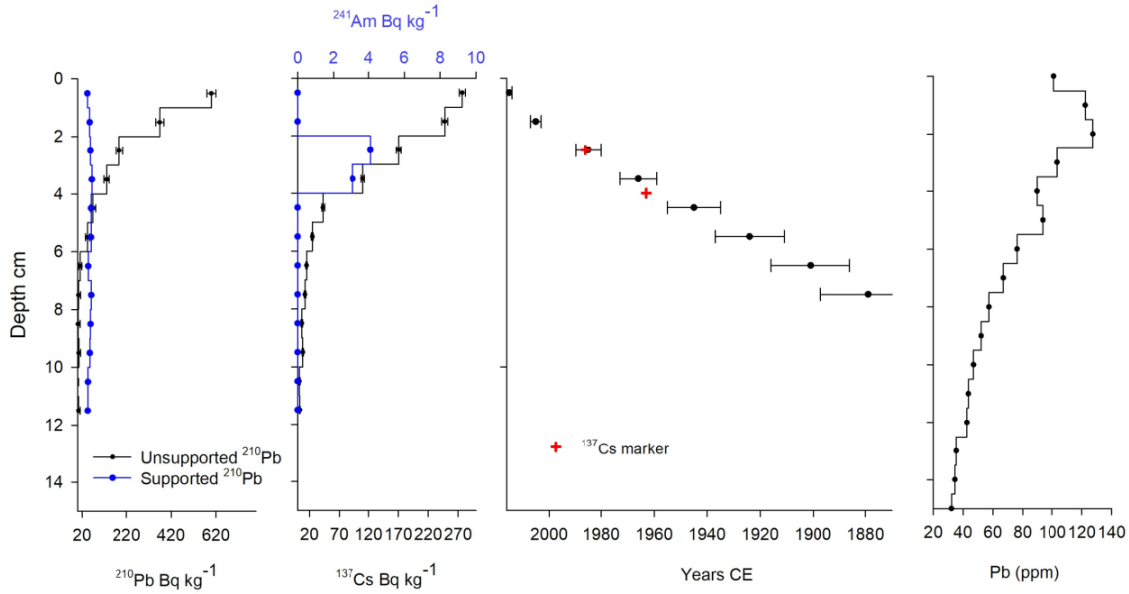

734

735 Figure 2: Radiometric chronology showing: a) concentrations of supported and unsupported

736 ^{210}Pb, b) concentrations of ^{137}Cs and ^{241}Am; c) the ^{210}Pb ages and the depths of the 1986

737 (Chernobyl) and post-1963 (weapons testing) ^{137}Cs and ^{241}Am markers. d) Airfall Pb pollutant

738 concentrations (determined by XRF).

739

740

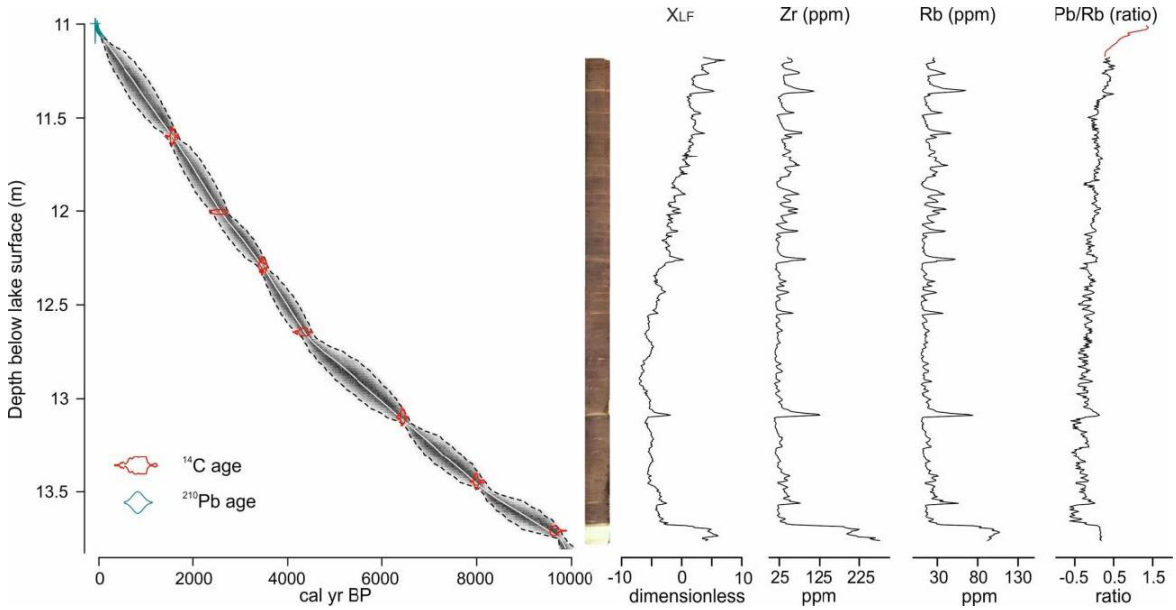

741

742 Figure 3. Age-depth model for Popradské pleso constructed using ^{210}Pb (light blue line near
743 modern) and 7 ^{14}C radiocarbon dates (shown in red) using 'BACON' (Blaauw and Christen,
744 2011). The gray area represents the 95th confidence intervals, and the white line delineates the
745 mean probability. High (µm) resolution digital line-scan image of the Pop15-1 core taken using
746 the University of Liverpool Geotek Multi-sensor core logger (MSCL-XZ). Down core profiles
747 for low frequency magnetic susceptibility (XLF), µXRF scan geochemical data for Zr (pmm), Rb
748 (ppm) and Pb/Rb for the long core. Pb/Rb ratio data continues to the modern period using dried
749 sample XRF measurements.

750

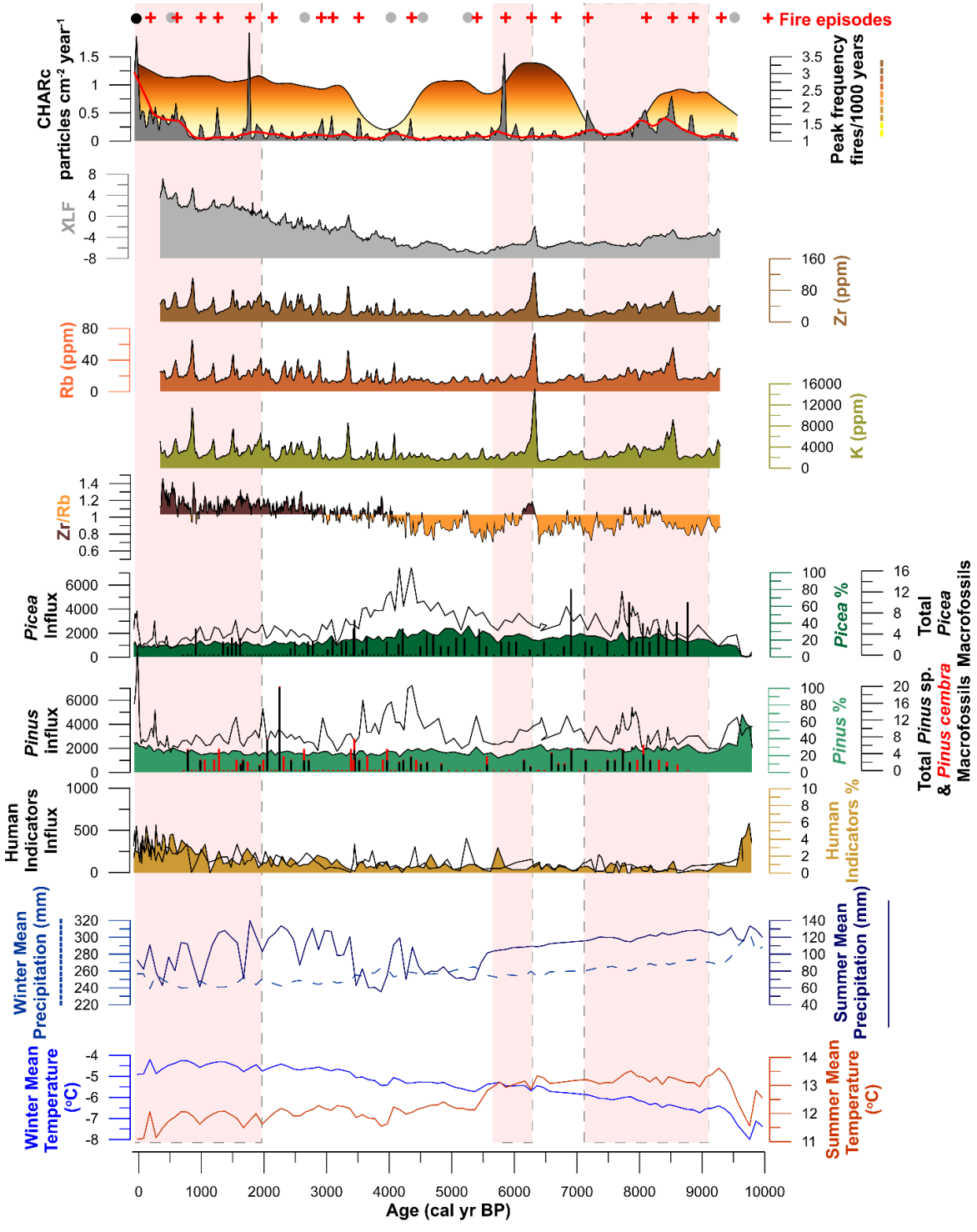

751

752 Figure 4. Reconstructed fire, geochemical, vegetation, and climate at Popradské pleso. From top

753 to bottom; Fire events are indicated with a red '+' symbol; less significant fire events are

delineated with a gray circle; Significant peaks identified by CharAnalysis, but are not true fire events are delineated with a black circle; $CHAR_C$ (particles per cm^{-2} yr^{-1}) (gray curve), with BCHAR (red line); fire frequency (fires/1000 years)(filled color curve); Magnetic susceptibility (XLF; gray filled curve); Zirconium (Zr; brown filled curve); Rubidium (Rb; reddish brown filled curve); Potassium (K; olive filled curve); Zr/Rb ratio (Zr = dark brown filled curve; Rb = orange filled curve); *Picea abies* pollen percentages (filled dark green curve), *Picea abies* pollen influx (black line), and *Picea abies* macrofossil concentrations (black vertical bars); *Pinus* pollen percentages (filled light green curve), *Pinus* pollen influx (black line), and *Pinus* sp. (black vertical bars) and *Pinus cembra* (red vertical bars) macrofossil concentrations; Human indicator taxa (i.e. the sum of primary and secondary anthropogenic pollen taxa) pollen percentages (filled orange curve), and human impact indicator species pollen influx (black line); MCM reconstructed summer temperature (red line); MCM reconstructed winter temperature (blue line); MCM reconstructed summer precipitation (dark blue line), MCM reconstructed winter precipitation (light blue dotted line). Pink vertical bars reflect the zones of significant biomass burning as indicated by change point analysis.

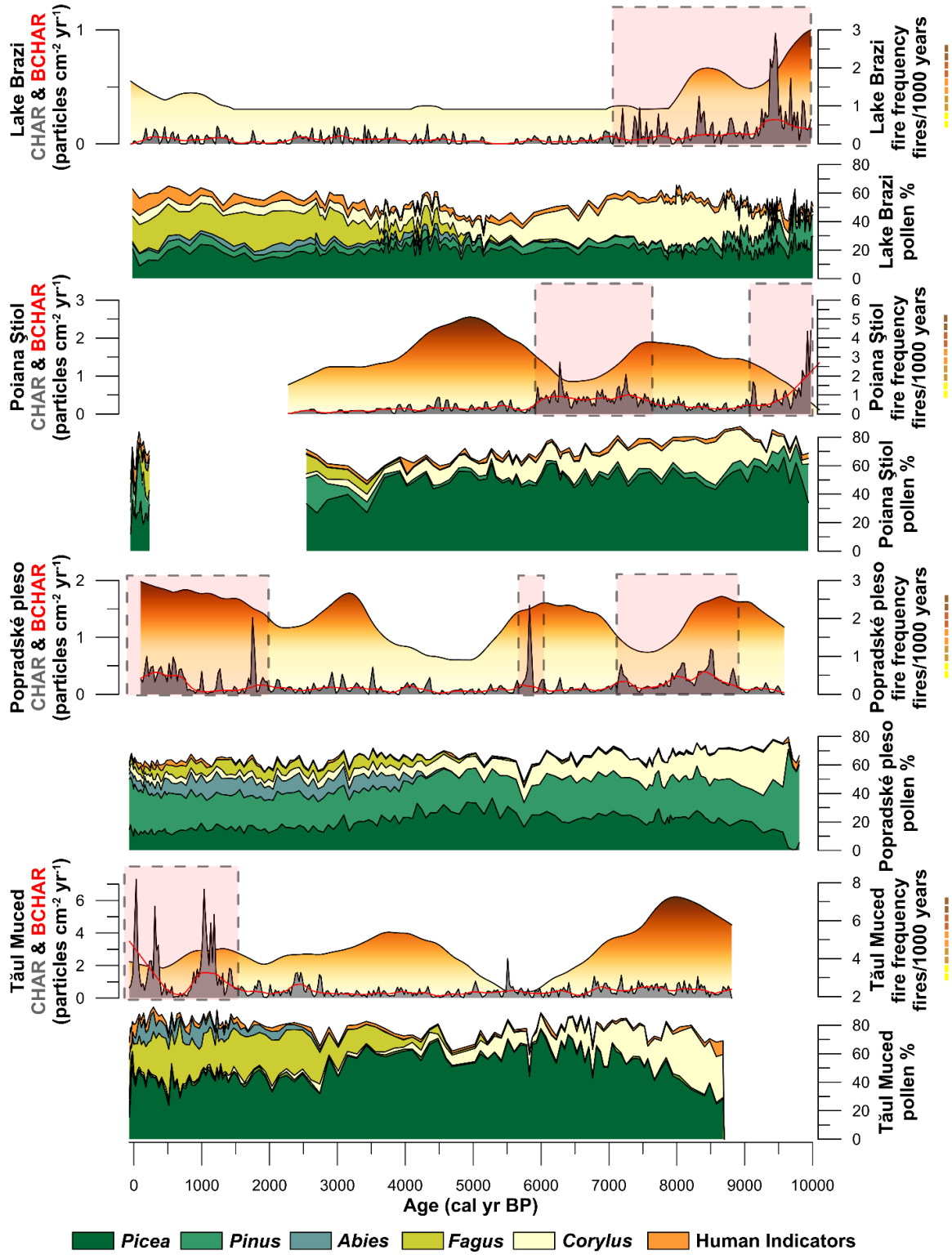
Lake Brazi
CHAR & BCHAR (particles cm-2 yr-1)
Lake Brazi fire frequency fires/1000 years
Lake Brazi pollen %
Poiana Ştiol
CHAR & BCHAR (particles cm-2 yr-1)
Poiana Ştiol fire frequency fires/1000 years
Poiana Ştiol pollen %
Popradské pleso
CHAR & BCHAR (particles cm-2 yr-1)
Popradské pleso fire frequency fires/1000 years
Popradské pleso pollen %
Tăul Muced
CHAR & BCHAR (particles cm-2 yr-1)
Tăul Muced fire frequency fires/1000 years
Tăul Muced pollen %
0 1000 2000 3000 4000 5000 6000 7000 8000 9000 10000
Age (cal yr BP)
Picea
Pinus
Abies
Fagus
Corylus
Human Indicators

770

771 Figure 5. Pan-Carpathian biomass burning and vegetation change at each of the four study sites
772 presented in this study; from top to bottom, Lake Brazi, elevation 1740 m a.s.l.; Poiana Ştiol,
773 elevation 1540 m a.s.l.; Popradské pleso, elevation 1513 m a.s.l.; Tăul Muced, elevation 1360 m
774 a.s.l. Biomass burning indicators are represented by both $CHAR_C$ and BCHAR (gray filled curve
775 and red line) and fire frequency (filled color curve). Vegetation change is represented by pollen
776 percentage data. Pink vertical bars reflect the zones of significant biomass burning as indicated
777 by change point analysis.

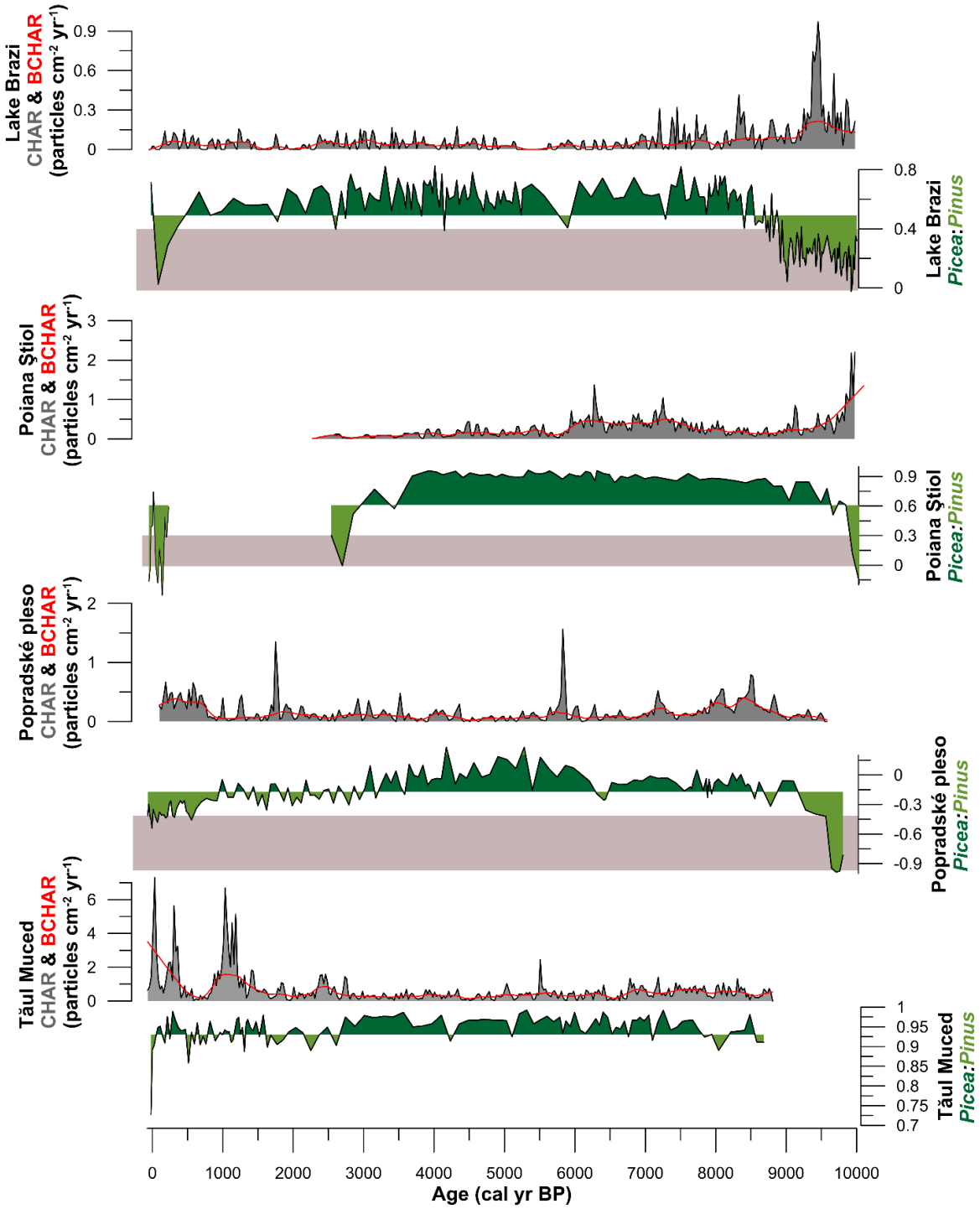

778

779 Figure 6. Figure illustrating how biomass burning ($CHAR_C$) increases (decreased) at all sites

780 when the forest cover is comprised with more *Pinus* (*Picea*); from top to bottom, Lake Brazi,

781 elevation 1740 m a.s.l.; Poiana Ştiol, elevation 1540 m a.s.l.; Popradské pleso, elevation 1513 m
782 a.s.l.; Tăul Muced, elevation 1360 m a.s.l. Horizontal gray bars on the *Picea:Pinus* curve
783 illustrate modeled values at which biomass burning increases (see Figure 7).
784
785
786
787
788
789
790
791
792

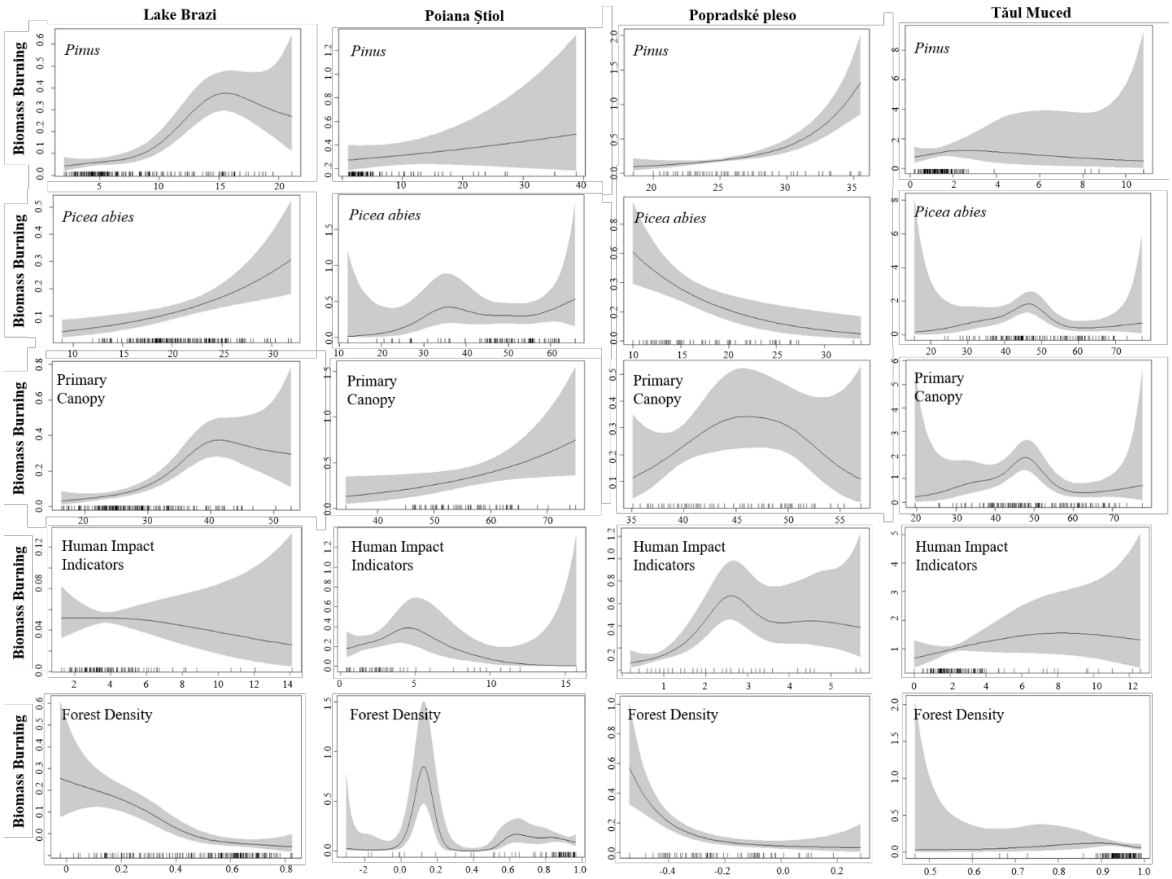

Figure 7. Generalized Additive Models showing the relationship between biomass burning (y-axis; $CHAR_C$) and dominant bottom-up drivers (from top to bottom, *Pinus*, *Picea*, primary canopy cover (sum of *Pinus* and *Picea*), human indicator species, and forest density (ratio of *Picea:Pinus*) at each of the four study sites shown from highest in elevation (Lake Brazi, left) to lowest in elevation (Tăul Muced, right). Pointwise confidence intervals (95%) are indicated by the gray bands.

Main Tables

Depth (cm)	Core ID	14C Age ± 1σb	Assigned 210Pb age (Year AD)	Assigned age (cal yr BP)	Material dated
1100	POP 15GC1		2015 ± 1	-65	
1101	POP 15GC1		2005 ± 2	-55	
1102	POP 15GC1		1985 ± 5	-35	
1103	POP 15GC1		1966 ± 7	-16	
1104	POP 15GC1		1945 ± 10	5	
1105	POP 15GC1		1924 ± 13	26	
1106	POP 15GC1		1901 ± 15	49	
1107	POP 15GC1		1879 ± 18	71	
1159.5	POP 15-1-1	1665 ± 35			*Picea abies* needle

Table 1. Radiocarbon (^{14}C) and ^{210}Pb dates used to constrain the depth-age relation for the Popradské pleso sediment sequence. Depths are presented by depth in centimeters below the water surface.

Site name	Independent variable	edf	ref.df	F value	p-value	Deviance explained
Lake Brazi	*Pinus*	3.78	4.71	26.35	0.001	44%
Lake Brazi	Primary Cover	3.53	4.42	19.53	0.001	36%
Lake Brazi	Forest Density	2.95	3.71	19.83	0.001	34%
Lake Brazi	*Picea abies*	1	1	11.91	0.001	8%
Lake Brazi	Human Indicators	1.41	1.72	0.47	0.682	1%
Poiana Ştiol	Forest Density	7.63	8.43	5.97	0.001	46%
Poiana Ştiol	Human Indicators	3.01	3.81	2.09	0.104	24%
Poiana Ştiol	Primary Cover	1.75	2.23	3.66	0.026	19%
Poiana Ştiol	*Picea abies*	3.59	4.51	0.96	0.45	16%

Table 2. Correlation between the independent variables, represented by pollen percentage data (*Pinus*, *Picea abies*, primary cover (i.e., the summed percentage values of *Picea abies* and *Pinus*,

816 forest density (the ratio of *Picea:Pinus*), and human indicator taxa) and the dependent variable
817 (biomass burning; charcoal influx) at each of the four study sites: from highest to lowest
818 elevation, Lake Brazi, Poiana Ştiol, Popradské pleso and Tăul Muced.
819
820
821
822
823
824
825
826
827
828
829
830
831
832
833
834
835
836
837
838

839

840 **SI Figures**

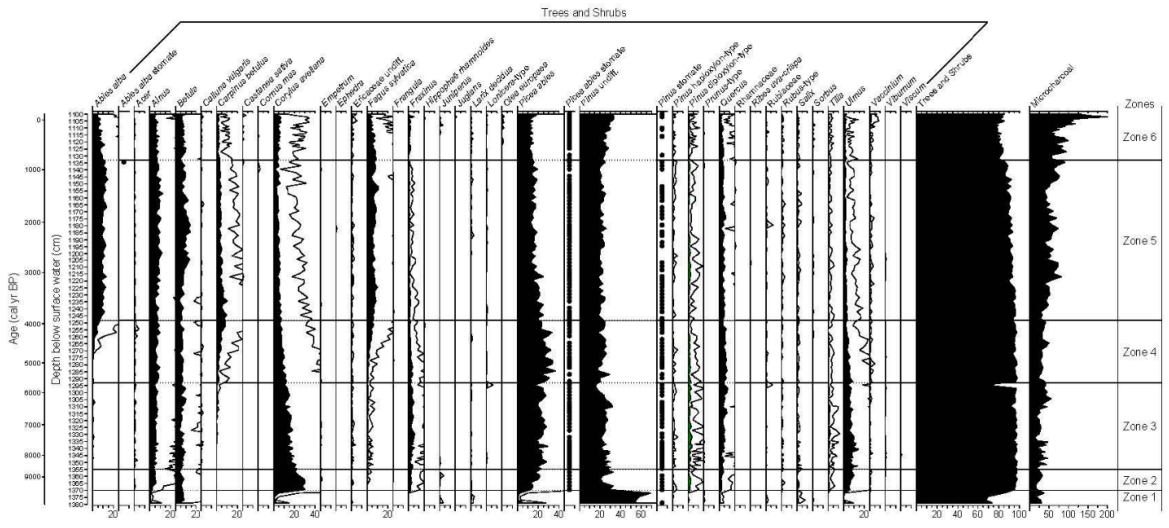

841

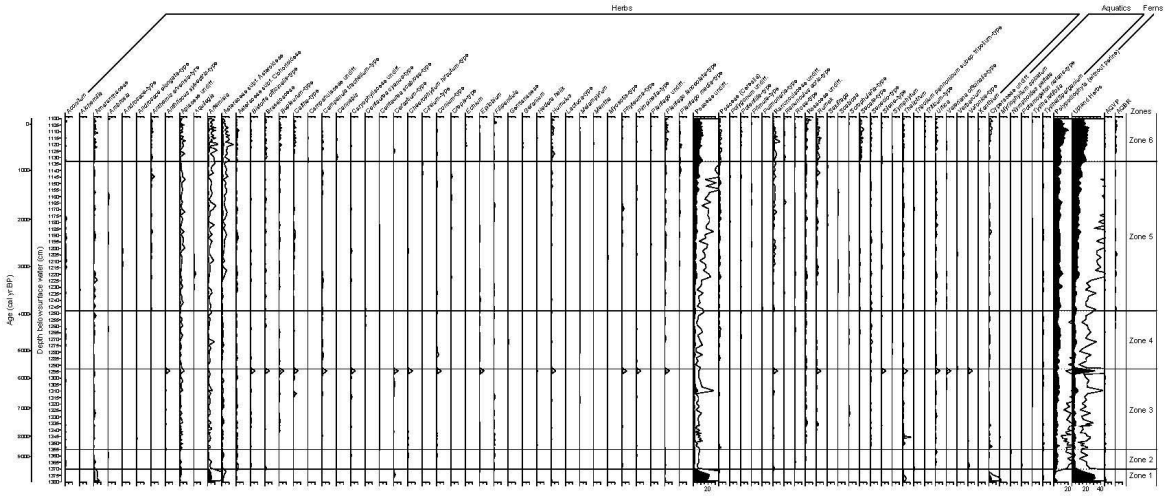

842

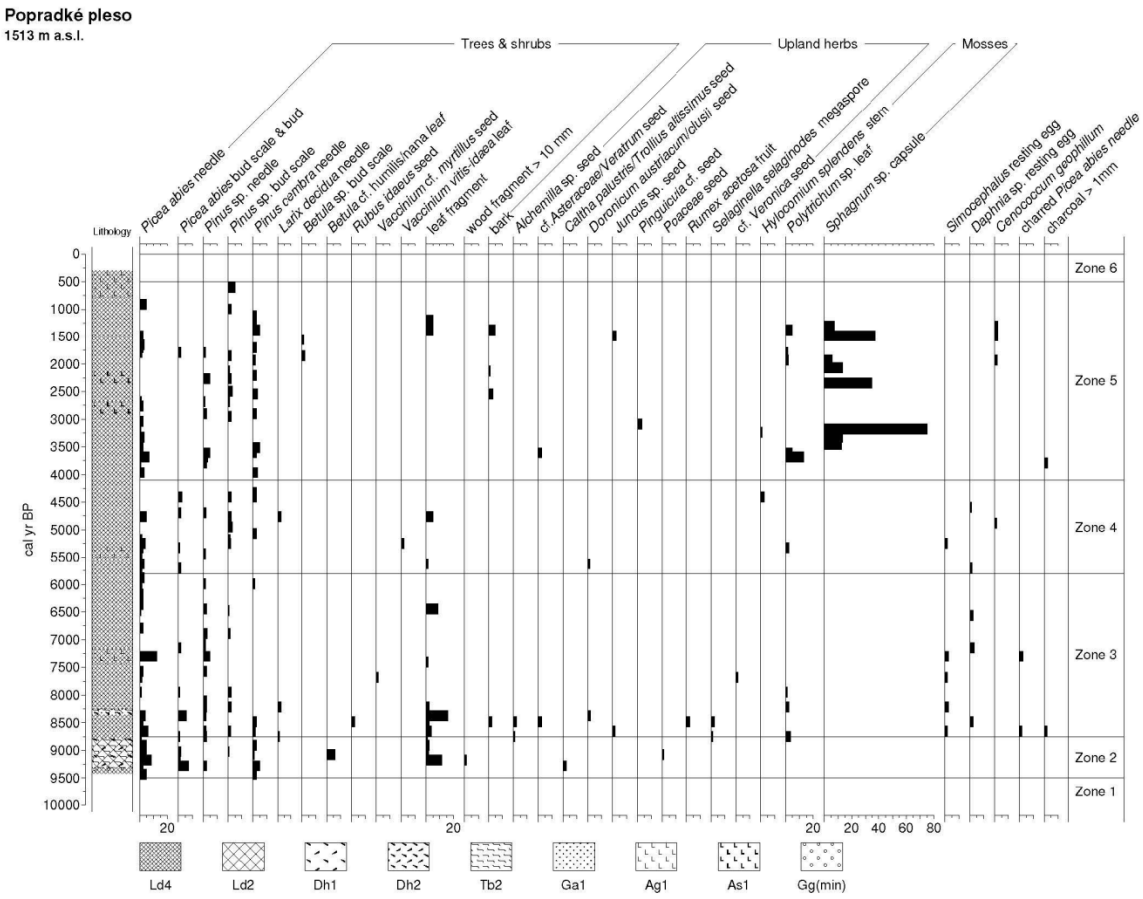

SI Figure 1. Pollen percentage diagrams (trees and shrubs on top, herbs in the middle figure), and macrofossil concentration diagram with core lithology (bottom) from Popradské pleso. Core lithology follows the Troels-Smith scheme (Troels-Smith, 1955).

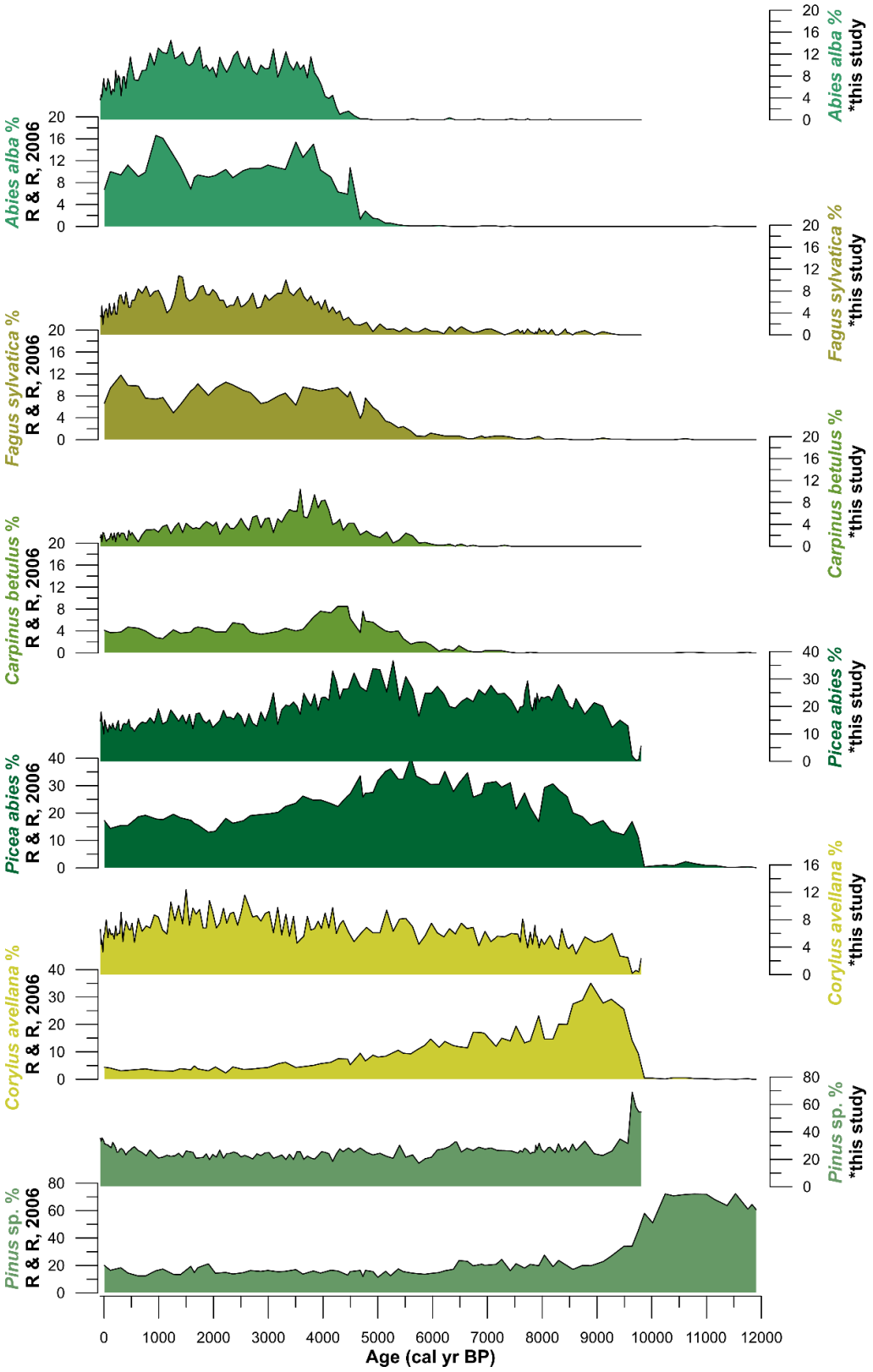
Abies alba %
R & R, 2006
Abies alba %
*this study
Fagus sylvatica %
R & R, 2006
Fagus sylvatica %
*this study
Carpinus betulus %
R & R, 2006
Carpinus betulus %
*this study
Picea abies %
R & R, 2006
Picea abies %
*this study
Corylus avellana %
R & R, 2006
Corylus avellana %
*this study
Pinus sp. %
R & R, 2006
Pinus sp. %
*this study
0 1000 2000 3000 4000 5000 6000 7000 8000 9000 10000 11000 12000
Age (cal yr BP)

848

849 SI Figure 2. Pollen percentage comparison between taxa identified by Rybníčková and Rybníček

850 (2006) and our study.

851

852

853 **SI Tables**

Site name	Human Indicator Species
Lake Brazi	Poaceae, Poaceae >40 mm, *Artemisia* , Chenopodiaceae, *Plantago lanceolata* , *Plantgao major-media* , *Plantago* sp., *Rumex acetosa /acetosella* , *Rumex* sp., *Polygonum aviculare* -type
Poiana Ştiol	Castaneae, *Juglans* , *Secale* -type, *Triticum* -type, Poaceae >40 mm, *Zea* , *Plantago lanceolata* , *Plantago media-type* , *Plantago* sp., *Rumex* sp., *Urtica* , *Linum* , Fabaceae, Polygonaceae, *Artemisia* sp., *Polygonium aviculare* , Chenopodiaceae, Brassicaceae, Asteraceae
Popradské pleso	*Secale* -type, *Triticum* -type, Poaceae >40mm, *Plantago lanceolata* , *Plantago media*- type, *Plantago* sp., *Rumex* sp.
Tăul Muced	Castaneae, *Juglans* , *Secale* -type, *Triticum* -type, Poaceae >40 mm, *Zea* , *Plantago lanceolata* , *Plantago media-type* , *Plantago* sp., *Rumex* sp., *Urtica* , *Linum* , Fabaceae, Polygonaceae, *Artemisia* sp., *Polygonium aviculare* , Chenopodiaceae, Brassicaceae, Asteraceae

854

855

856

SI Table 1. List of taxa used to calculate an index of human indicators at each of the four study sites: from highest to lowest elevation, Lake Brazi, Poiana Ştiol, Popradské pleso and Tăul Muced.

References

Abraham, V., Kuneš, P., Petr, L., Svitavská-Svobodová, H., Kozáková, R., Jamrichová, E., Švarcová, M.G., Pokorný, P., 2016. A pollen-based quantitative reconstruction of the Holocene vegetation updates a perspective on the natural vegetation in the Czech Republic and Slovakia. Preslia 88, 409–434.

Achard, F., Eva, H., Mollicone, D., Popatov, P., Stibig, H.-J., Turubanova, S. & Yaroshenko, A., 2009. Detecting intact forests from space: hot spots of loss, deforestation and the UNFCCC. In: Old-Growth Forests, ed. C. Wirth, G. Gleixner & M. Heimann, Berlin and Heidelberg, Germany: Springer. pp. 411–427.

Alberton, M., Andresen, M., Citadino, F., Egerer, H., Fritsch, U., Götsch, H., Hoffmann, C., Klemm, J., Mitrofanenko, A., Musco, E., Noellenburg, N., Pettita, M., Renner, K., Zebisch, M., 2017. Outlook on climate change adaptation in the Carpathian Mountains. United Nations Environment Programme, GRID-Arendal and Eurac Research, Nairobi, Vienna, Arendal and Bolzano.

878 Albrich, K., Rammer, W., Thom, D., Seidl, R., 2018. Trade-offs between temporal stability and
879 level of forest ecosystem services provisioning under climate change. Ecological Applications 28
880 (7), 1884–1896.
881
882 Ali, A.A., Carcaillet, C., Talon, B., Roiron, P. and Terral, J-F., 2005. Pinus cembra L. (arolla
883 pine), a common tree in the inner French Alps since the early Holocene and above the present
884 tree line: a synthesis based on charcoal data from soils and travertines. Journal of Biogeography
885 32, 1659–1669.
886
887 Anders, I., Stagl, J., Ingeborg, A., Pavlik, D., 2014. Climate Change in Central and Eastern
888 Europe. In. Rannow S., Neubert M. (eds) Managing Protected Areas in Central and Eastern
889 Europe Under Climate Change. Advances in Global Change Research, vol 58. Springer,
890 Dordrecht.
891
892 Appleby, P.G., Oldfield, F., 1978. The calculation of lead-210 dates assuming a constant rate of
893 supply of unsupported 210Pb to the sediment. Catena 5, 1–8.
894
895 Appleby, P.G., Nolan, P.J., Gifford, D.W., Godfrey, M.J., Oldfield, F., Anderson, N.J.,
896 Batterbee, R.W., 1986. 210Pb dating by low background gamma counting. Hydrobiologia 143,
897 21–27.
898

Appleby, P.G., Richardson, N., Nolan, P.J., 1992. Self-absorption corrections for well-type germanium detectors. Nuclear Instruments and Method in Physics Research Section B 71, 228–233.

Auer, I., Böhm, R., Jurkovic, A., Lipa, W., Orlik, A., Potzmann, R., Schöner, W., Ungersböck, M., Matulla, C., Briffa, K., Jones, P.D., Efthymiadis, D., Brunetti, M., Nanni, T., Maugeri, M., Mercalli, L., Mestre, O., Moisselin, J-M., Begert, M., Müller-Westermeier, G., Kveton, V., Bochnicek, O., Stastny, P., Lapin, M., Szalai, S., Szentimrey, T., Cegnar, T., Dolinar, M., Gajic-Capka, M., Zaninovic, K., Majstorovic, Z., Nieplova, E., 2007. HISTALP—Historical instrumental climatological surface time series of the greater. Alpine region 1760–2003. International Journal of Climatology 27, 17–46.

Barhoumi, G., Peyron, O., Joannin, S., Subetto, D., Kryshen, A., Drobyshev, I., Girardin, M., Brossier, B., Paradis, L., Pastor, T., Alleaume, S., Ali, A.A., 2019. Gradually increasing forest fire activity during the Holocene in the northern Ural region (Komi Republic, Russia). The Holocene 29(12), 1906–1920.

Bennett, K.D., 1996. Determination of the number of zones in a biostratigraphical sequence. New Phytologist 132 (1), 155–170.

Berger, A., Loutre, M.F., 1991. Insolation value for the climate of the last 10 million years. Quaternary Science Reviews 10, 297–317.

922 Berthel, N., Schwörer, C., Tinner, W., 2012. Impact of Holocene climate changes on alpine and
923 treeline vegetation at Sanetsch Pass, Bernese Alps, Switzerland. Review of Palaeobotany and
924 Palynology 174, 91–100.
925
926 Beug, H.-J., 2004. Leitfaden der Pollenbestimmung für Mitteleuropa und angrenzende Gebiete.
927 Verlag Dr Friedrich Pfeil, Munich.
928
929 Birks, H.J.B., and Gordon, A.D., 1985. Numerical Methods in Quaternary Pollen Analysis.
930 Academic Press, London.
931
932 Birks, H.H., 2007. Plant macrofossil introduction. In: Elias, S.A. (ed.) Encyclopedia of
933 Quaternary Science, Volume 3. Elsevier, Amsterdam, 2266–2288.
934
935 Blaauw, M., and Christen, J.A., 2011. Flexible paleoclimate age-depth models using an
936 autoregressive gamma process. Bayesian Analysis 6, 457–474.
937
938 Blarquez, O., and Carcaillet, C., 2010. Fire, fuel composition and resilience threshold in
939 subalpine ecosystem. PLoS ONE 5(8), e13480.
940
941 Bogdan, O., 2008. Carpaţii Meridionali. Clima, hazardele meteo - Climatice şi impactul lor
942 asupra dezvoltarii turismului. In: Academia Română., Institutul de Geografie. Univ., Lucian
943 Blaga, Sibiu, Romania (In Romanian), pp. 1–314.
944

945 Bojňanský, V., Fargašová, A., 2007. Atlas of Seeds and Fruits of Central and East-European
946 Flora. The Carpathian Mountains Region. Springer, Dordrecht.
947
948 Boyle, J.F., 1995. A simple closure mechanism for a compact, large-diameter, gravity corer.
949 Journal of Paleolimnology 13 (1), 85–87.
950
951 Boyle, J.F., 2001. Inorganic geochemical methods in palaeolimnology. In: Last WM, Smol JP
952 (eds) Tracking environmental change using lake sediments. Volume 2: physical and geochemical
953 methods. Kluwer Academic Publishers, Dordrecht, pp 83–141.
954
955 Boyle, J.F., Chiverrell, R.C., Schillereff, D.N., 2015. Approaches to water content correction and
956 calibration for μXRF core scanning: comparing x-ray scatter with simple regression of elemental
957 concentrations, in: Rothwell, R.G., Croudace, I.W. (Eds.), Developments in Palaeoenvironmental
958 Research: Micro-XRF Studies of Sediment Cores. Springer, Dordrecht.
959
960 Brown, T.A., Nelson, D.E., Mathewes, R.W., Vogel, J.S., Southon, J.R., 1989. Radiocarbon
961 dating of pollen by accelerator mass spectrometry. Quaternary Research 32, 205–212.
962
963 Bryson, R., 2005. Archeoclimatology. Encyclopedia of World Climatology. Springer,
964 Netherlands, pp. 58–63.
965
966 Cappers, R.T.J., Bekker, R.M., Jans, J.E.A., 2006. Digitale Zadenatlas van Nederland,

967 Groningen Archaeological Studies, vol. 4. Barkhuis Publishing & Groningen University Library,
968 Groningen.
969
970 Caudullo, G., Tinner, W., de Rigo, D., 2016. Picea abies in Europe: distribution, habitat, usage
971 and threats. In: San-Miguel-Ayanz, J., de Rigo, D., Caudullo, G., Houston Durrant, T., Mauri, A.
972 (Eds.), European Atlas of Forest Tree Species. Publ. Off. EU, Luxembourg.
973
974 Chen, J., Saunders, S.C., Crow, T.R., Naiman, R.J., Brosofske, K.D., Mroz, G.D., Brookshire,
975 B.L., Franklin, J.F., 1999. Microclimate in forest ecosystem and landscape ecology: variations in
976 local climate can be used to monitor and compare the effects of different management regimes.
977 BioScience 49, 288–298.
978
979 Chiverrell, R. C., Sear, D., Warburton, J., Macdonald, N., Schillereff, D.N, Dearing, J.A.,
980 Bradley, J., 2019. Using lake sediment archives to improve understanding of flood magnitude
981 and frequency: Recent extreme flooding in northwest UK. Earth Surface Processes and
982 Landforms, 44(12), 2366–2376.
983
984 Clark, J.S., Royall, P.D., 1995. Particle size evidence for source areas of charcoal accumulation
985 in late Holocene sediments of eastern North American lakes. Quaternary Research 43, 80–89.
986
987 Clear, J.L., Molinari, C., Bradshaw, R.H.W., 2014. Holocene fire in Fennoscandia and Denmark.
988 International Journal of Wildland Fire 23, 781–789.
989

990 Colombaroli, D., Henne, P.D., Kaltenrieder, P., Gobet, E., Tinner, W., 2010. Species response to
991 fire, climate and human impact at tree line in the Alps as evidenced by palaeo-environmental
992 records and a dynamic simulation model. Journal of Ecology 98, 1346–1357.
993
994 Courtney-Mustaphi, C.J., Pisaric, M.F.J., 2013. Varying influences of climate and aspect as
995 controls of montane forest fire regimes during the late Holocene, south-eastern British Columbia,
996 Canada. Journal of Biogeography 40, 1983–1996.
997
998 Czerwiński, S., Margielewski, W., Gałka, M, Kołaczek, P., 2019. Late Holocene transformations
999 of lower montane forest in the Beskid Wyspowy Mountains (Western Carpathians, Central
1000 Europe): a case study from Mount Mogielica. Palynology 44(2), 355–368.
1001
1002 Davies, S., Lamb, H., Roberts, S. J., 2015. Micro-XRF Studies of Sediment Cores: Applications
1003 of a non-destructive tool for the environmental sciences. Springer Nature, Vol. 17. p. 189-226 38
1004 p. (Developments in Paleoenvironmental Research; vol. 17).
1005
1006 Davis, K.T., Dobrowski, S.Z., Holden, Z.A., Higuera, P.E., Abatzoglou, J.T., 2018. Microclimate
1007 buffering in forests of the future: the role of local water balance. Ecography 42, 1–11.
1008
1009 Dearing, J.A., 1992. Sediment yields and sources in a Welsh upland lake-catchment during the
1010 past 800 years. Earth Surf Process Landf 17:1–22
1011

1012 Diaconu, A.-C., Tóth, M., Lamentowicz, M., Heiri, O., Kuske, E., Tanţău, I., Panait, A.-M.,
1013 Braun, M., Feurdean, A., 2017. How warm? How wet? Hydroclimate reconstruction of the past
1014 7500 years in northern Carpathians, Romania. Palaeogeography, Palaeoclimatology,
1015 Palaeoecology 482, 1–12.
1016
1017 Dietre, B., Walser, C., Kofler, W., Kothieringer, K., Hajdas, I., Lambers, K., Reitmaier, T., Haas,
1018 J.N., 2016. Neolithic to Bronze Age (4850-3450 cal. BP) fire management of the Alpine Lower
1019 Engadine landscape (Switzerland) to establish pastures and cereal fields. The Holocene 27, 181–
1020 196.
1021
1022 Dietze, E., Theuerkauf, M., Bloom, K., Brauer, A., Dörfler, W., Feeser, I., Feurdean, A.,
1023 Gedminienė, L., Giesecke, T., Jahns, S., Karpińska-Kołaczek, M., Kołaczek, P., Lamentowicz,
1024 M., Latałowa, M., Marcisz, K., Obremska, M., Pędziszewska, A., Poska, A., Rehfeld, K.,
1025 Stančikaitė, M., Stivrins, N., Święta-Musznicka, J., Szal, M., Vassiljev, J., Veski, S., Wacnik, A.,
1026 Weisbrodt, D., Wiethold, J., Vannière, B., Słowiński, M., 2018. Holocene fire activity during
1027 low-natural flammability periods reveals scale-dependent cultural human-fire relationships in
1028 Europe. Quaternary Science Reviews 201, 44–56.
1029
1030 Dragotă, C.S., and Kucsisca, G., 2011. Global climate change-related particularities in the
1031 Rodnei Mountains National Park. Carpathian Journal of Earth and Environmental Sciences 6 (1),
1032 43–50.
1033

1034 Faegri, K., Kaland, P.E., Kzywinski, K., 1989. Textbook of Pollen Analysis. Wiley, New York.
1035 pp 1–3237.
1036
1037 Fărcaş, S., Tanţău, I., Bodnariuc, A., 2003. The Holocene human presence in Romanian
1038 Carpathians, revealed by the palynological analysis. Wurzburger Geographische Manuskripte,
1039 63, 111–128.
1040
1041 Fărcaş, S., Tanţău, I., Mîndrescu, M., Hurdu, B., 2013. Holocene vegetation history in the
1042 Maramureş Mountains (Northern Romanian Carpathians). Quaternary International 293, 92–104.
1043
1044 Feurdean, A., Klotz, S., Mosbrugger, V., Wohlfarth, B., 2008. Pollen-based quantitative
1045 reconstructions of Holocene climate variability in NW Romania. Palaeogeography,
1046 Palaeoclimatology, Palaeoecology 260, 494–504.
1047
1048 Feurdean, A., Tanţău, I., Fărcaş, S., 2011. Holocene variability in the range distribution and
1049 abundance of Pinus, Picea abies, and Quercus in Romania; implications for their current status.
1050 Quaternary Science Reviews, 30, 3060–3075.
1051
1052 Feurdean, A., Spessa, A., Magyari, E.K.,Veres, D.,Hickler, T., 2012. Trends in biomass burning
1053 in the Carpathian region over the last 15,000 years. Quaternary Science Reviews 45, 111–125.
1054

1055 Feurdean, A., Liakka, J., Vannière, B., Marinova, E., Hutchinson, S.M., Mosburgger, V.,
1056 Hickler, T., 2013. 12,000-Years of fire regime drivers in the lowlands of Transylvania (Central-
1057 Eastern Europe): a data-model approach. Quaternary Science Reviews 81, 48–61.
1058
1059 Feurdean, A., Galka, M., Kuske, E., Tanţău, I., Lamentowicz, M., Florescu, G., Liakka, J.,
1060 Hutchinson, S.M., Mulch, A., Hickler, T., 2015. Last Millennium hydro-climate variability in
1061 Central-Eastern Europe (Northern Carpathians, Romania). The Holocene 25, 1179–1192.
1062
1063 Feurdean, A., Gałka, M., Tanţău, I, Geantă, A., Hutchinson, S.M., Hickler, T., 2016. Tree and
1064 timberline shifts in the northern Romanian Carpathians during the Holocene and the responses to
1065 environmental changes. Quaternary Science Reviews 134, 100–113.
1066
1067 Feurdean, A., Florescu, G., Vannière, B., Tanţău, I. O'Hara, R.B., Pfeiffer, M., Hutchinson,
1068 S.M., Gałka, M., Moskal-del Hoyo, M., Hickler, T., 2017. Fire has been an important driver of
1069 forest dynamics in the Carpathian Mountains during the Holocene. Forest Ecology and
1070 Management 389, 15–26.
1071
1072 Feurdean, A., Vannière, B., Finsinger, W., Liakka, J., Panait, A., Warren, D., Connor, S., Forrest,
1073 M., Werner, C., Andrič, M., Bobek, P., Carter, V.A., Davis, B., Diaconu, A., Dietze, E., Feeser,
1074 I., Florescu, G., Gałka, M., Giesecke, T., Jahns, S., Jamrichová, E., Kajukało, K., Kaplan, J.,
1075 Karpińska-Kołaczek, M., Kołaczek, P., Kuneš, P., Kupriyanov, D., Lamentowicz, M.,
1076 Lemmen, C., Maryari, E., Marcisz, K., Marinova, E., Rösch, M., Słowiński, M., Stančikaité,
1077 M., Szal, M., Święta-Musznicka, J., Tanţău, I., Theuerkauf, M., Tonkov, S., Valkó, O., Vassiljev,

1078 J., Veski, S., Vincze, I., Wacnik, A., Wiethold, J., Hickler, T., Niamir, A., Novenko, E.,
1079 Obremska, M., Pędziszewska, A., Pfeiffer, M., Poska, A., 2020. Fire risk modulation by forest
1080 structure and land use in Eastern and Central Europe. Biogeosciences. 71(5), 1213–1230.
1081
1082 Field, C.B., Barros, V.R., Mach, K.J., Mastrandrea, M.D., van Aalst, M., Adger, W.N., Arent,
1083 D.J., Barnett, J., Betts, R., Bilir, T.E., Birkmann, J., Carmin, J., Chadee, D.D., Challinor, A.J.,
1084 Chatterjee, M., Cramer, W., Davidson, D.J., Estrada, Y.O., Gattuso, J.P., Hijioka, Y., Hoegh-
1085 Guldberg, O., Huang, H.Q., Insarov, G.E., Jones, R.N., Kovats, R.S., Romero-Lankao, P.,
1086 Larsen, J.N., Losada, I.J., Marengo, J.A., McLean, R.F., Mearns, L.O., Mechler, R., Morton, J.F.,
1087 Niang, I., Oki, T., Olwoch, J.M., Opondo, M., Poloczanska, E.S., Pörtner, H.O., Redsteer, M.H.,
1088 Reisinger, A., Revi, A., Schmidt, D.N., Shaw, M.R., Solecki, W., Stone, D.A., Stone, J.M.R.,
1089 Strzepek, R.M., Suarez, A.G., Tschakert, P., Valentini, R., Vicuña, S., Villamizar, A., Vincent,
1090 K.E., Warren, R., White, L.L., Wilbanks, T.J., Wong, P.P., Yohe, G.W., 2014. Technical
1091 summary. In: Climate Change 2014: Impacts, Adaptation, and Vulnerability. Part A: Global and
1092 Sectoral Aspects. Contribution of Working Group II to the Fifth Assessment Report of the
1093 Intergovernmental Panel on Climate Change [Field, C.B., V.R. Barros, D.J. Dokken, K.J. Mach,
1094 M.D. Mastrandrea, T.E. Bilir, M. Chatterjee, K.L. Ebi, Y.O. Estrada, R.C. Genova, B. Girma,
1095 E.S. Kissel, A.N. Levy, S. MacCracken, P.R. Mastrandrea, and L.L.White (eds.)]. Cambridge
1096 University Press, Cambridge, United Kingdom and New York, NY, USA, pp. 35-94.
1097
1098 Finsinger, W., Kelly, R., Fevre, J., Magyari, E.K., 2014. A guide to screening charcoal peaks in
1099 macrocharcoal-area records for fire-episode reconstructions. The Holocene 24(8), 1002–1008.
1100

1101 Finsinger, W., Fevre, J., Orbán, I., Pál, I., Vincze, I., Hubay, K., Birks, H.H., Braun, M., Tóth,
1102 M., Magyari, E.K., 2018. Holocene fire-regime changes near the treeline in the Retezat Mts.
1103 (Southern Carpathians, Romania). Quaternary International 477, 94–105.
1104
1105 Flachbart, V., 2007 Bezbukové oblasti na Slovensku – skutočnosť alebo fikcia? – In: RIZMAN I.
1106 (ed.): Lesnícka typológia a zisťovanie stavu lesa vo väzbe na trvalo udržateľné
1107 obhospodarovanie lesov : Zborník príspevkov a prezentácií z odborného seminára konaného 3.
1108 12. 2007 na NLC vo Zvolene v elektronickej forme [CD-ROM]. NLC – Ústav lesných zdrojov a
1109 informatiky, Zvolen.
1110
1111 Florescu, G., Vannière, B., Feurdean, A., 2018. Exploring the influence of local controls on fire
1112 activity using multiple charcoal records from northern Romanian Carpathians. Quaternary
1113 International 488, 41–57.
1114
1115 Florescu, G., Brown, K.J., Carter, V.A., Kuneš, P., Veski, S., Feurdean, A., 2019. Holocene
1116 rapid climate changes and ice-rafting debris events reflected in high-resolution European
1117 charcoal records. Quaternary Science Reviews 222, 105877.
1118
1119 Fyfe, R.M., Woodbridge, J., Roberts, N., 2015. From forest to farmland: pollen-inferred land
1120 cover change across Europe using the pseudobiomization approach. Global Change Biology
1121 21(3), 1197–1212.
1122

1123 Gałka, M., Tanţău, I., Ersek, V., Feurdean, A., 2016. A 9000 year record of cyclic vegetation
1124 changes identified in a montane peatland deposit located in the Eastern Carpathians (Central-
1125 Eastern Europe): autogenic succession or regional climatic influences? Palaeogeography,
1126 Palaeoclimatology, Palaeoecology 449, 52–61.
1127
1128 Gałka, M., Tanţău, I., Carter, V.A., Feurdean, A., 2020. The Holocene dynamics of moss
1129 communities in subalpine wetland ecosystems in the Eastern Carpathian Mountains, Central
1130 Europe. The Bryologist 123(1), 84–97.
1131
1132 Gavin, D.G., Hu, F.S., Lertzman, K., Corbett, P., 2006. Weak climatic control of standscale fire
1133 history during the late Holocene. Ecology 87, 1722–1732.
1134
1135 Geantă, A., Gałka, M., Tanţău, I., Hutchinson, S., Mîndrescu, M., Feurdean, A., 2014. High
1136 mountain region of the Northern Romanian Carpathians responded sensitively to Holocene
1137 climate and land use change: A multi-proxy analysis. The Holocene 24(8), 944–956.
1138
1139 Genries, A., Mercier, L., Lavoie, M., Muller, S.D., Radakovitch, O., Carcaillet, O., 2009. The
1140 effect of fire frequency on local Cembra Pine populations. Ecology 90(2), 476–486.
1141
1142 Gottfried, M., Pauli, H., Futschik, A., Akhalkatsi, M., Barančok, P., Alonso, J.L.B., Coldea, G.,
1143 Dick, J., Erschbamer, B., Calzado, M.R.F., Kazakis, G., Krajči, J., Larsson, P., Mallaun, M.,
1144 Michelsen, O., Moiseev, D., Moiseev, P., Molau, U., Merzouki, A., Nagy, L., Nakhutsrishvilli,
1145 G., Pedersen, B., Pelino, G., Puscas, M., Rossi, G., Stanisci, A., Theurillat, J-P., Tomaselli, M.,

1146 Villar, L., Vittoz, P., Vogiatzakis, I., Grabherr, G., 2012. Continent-wide response of mountain
1147 vegetation to climate change. Nature Climate Change 2, 111–115.
1148
1149 Gray, J., 1965 Extraction techniques. In Kummel, B. and Raup, G., eds., Handbook of
1150 Palaeontological Techniques. San Francisco, W. H. Freeman & Co.: 530–587.
1151
1152 Greenwood, S., Jump, A.S., 2014. Consequences of treeline shifts for the diversity and function
1153 of high altitude ecosystems. Arctic Antarctic and Alpine Research 46, 829–840.
1154
1155 Grindean, R., Tanţău, I., Feurdean, A., 2019. Linking vegetation dynamics and stability in old-
1156 growth forests of Central Eastern Europe: Implications for forest conservation and management.
1157 Biological Conservation 229, 160–169.
1158
1159 Grodzińska, K., Godzik, B., Frączek, W., Badea, O., Oszlányi, J., Postelnicu, D., Shparyk, Y.,
1160 2004. Vegetation of the selected forest stands and land use in the Carpathian Mountains.
1161 Environmental Pollution 130, 17–32.
1162
1163 Hájková, P., Grootjans, A.B., Lamentowicz, M., Rybníčková, E., Madaras, M., Opravilová, V.,
1164 Michaelis, D., Hájek, M., Joosten, H., Wołejko, L., 2012. How a *Sphagnum fuscum*-dominated
1165 bog changed into a calcareous fen: the unique Holocene history of a Slovak spring-fed mire.
1166 Journal of Quaternary Science 27(3), 233–243.
1167

1168 Hájková, P., Pařil, P., Petr, L., Chattová, B., Matys Grygar, T., Heiri, O., 2016. A first
1169 chironomid-based summer temperature reconstruction (13–5 ka BP) around 49ºN in inland
1170 Europe compared with local lake development. Quaternary Science Reviews 141, 94–111.
1171
1172 Harsch, M.A., Hulme, P.E., McGlone, M.S., Duncan, R.P., 2009. Are treelines advancing? A
1173 global meta-analysis of treeline response to climate warming. Ecology Letters 12(10), 1040–
1174 1049.
1175
1176 Hastie, T.J., Tibshirani, R.J., 1986. Generalized additive models. Statistical Science 1(3), 297–
1177 318.
1178
1179 Henne, P., Elkin, C.M., Reineking, B., Bugmann, H., Tinner, W., 2011. Did soil development
1180 limit spruce (*Picea abies*) expansion in the Central Alps during the Holocene? Testing a
1181 palaeobotanical hypothesis with a dynamic landscape model. Journal of Biogeography 38(5),
1182 933–949.
1183
1184 Hess, M., 1965. Piętra klimatyczne w polskich Karpatach Zachodnich (Vertical climatic zones in
1185 the Polish Western Carpathians). Zesz Nauk UJ Pr Geograficzne 11, 1–267 (in Polish).
1186
1187 Hess, M., 1974 Piętra klimatyczne w Tatrach (Vertical climatic zones in the Tatra Mountains).
1188 Czasopismo Geograficzne 45, 75–95 (in Polish, English summary).
1189
1190 Higuera, P.E., Brubaker, L.B., Anderson, P.M., Hu, F.S., Brown, T., 2009. Vegetation mediated

1191 the impacts of postglacial climate change on fire regimes in the south-central Brooks Range,
1192 Alaska. Ecological Monographs 79, 201–219.
1193
1194 Higuera, P.E., Gavin, D.G., Bartlein, P.J., Hallett, D.J., 2010. Peak detection in
1195 sediment–charcoal records: impacts of alternative data analysis methods on fire-history
1196 interpretations. International Journal of Wildland Fire. 19, 996–1114.
1197
1198 Higuera, P.E., Briles, C.E., Whitlock, C., 2014. Fire-regime complacency and sensitivity to
1199 centennial through millennial-scale climate change in Rocky Mountain subalpine forests,
1200 Colorado, USA. Journal of Ecology 102, 1429–1441.
1201
1202 Hlásny, T., and Sitková, Z., 2010. Spruce forests decline in the Beskids. National Forest
1203 Centre—Forest Research Institute Zvolen, Czech University of Life Sciences Prague, Forestry
1204 and Game Management Research Institute Jíloviště–Strnady, Zvolen, Slovakia. pp. 1–165.
1205
1206 Jamrichová, E., Gálová, A., Gašpar, A., Horsák, M., Frodlová, J., Hájek, M., Hajnalová, M.,
1207 Hájkova, P., 2018. Holocene development of two calcareous spring gens at the Carpathian-
1208 Pannonian interface controlled by climate and human impact. Folia Geobotanica 53, 243–263.
1209
1210 Jankovská, V. 1972. Pyloanalytický příspěvek ke složení původních lesů v severozápadní části
1211 Spišské kotliny. Biológia 27, 279–292.
1212

1213 Jawor, G., 2016a. Northern extent of settlement on the Wallachian law in medieval Poland. Res
1214 Historica 41, 35–49.
1215
1216 Jawor, G., 2016b. Seasonal pastoral exploitation of forests in the area of Subcarpathia in the 15th
1217 and 16th century. Balcanica Posnaniensia 23, 175–185.
1218
1219 Katz, N.J., Katz, S.V., Skobeeva, E.I., 1977. Atlas of Plant Remains in Peat. Nedra, Moscow.
1220
1221 Kelly, R.F., Higuera, P.E., Barrett, C.M., Hu, F.S., 2011. A signal-to-noise index to quantify the
1222 potential for peak detection in sediment–charcoal records. Quaternary Research 75, 11–17.
1223
1224 Kertész, R., 2002. Mesolithic hunter-gatherers in the northwestern part of the great Hungarian
1225 Plain. Praehistoria 3, 281–304.
1226
1227 Killick, R., Eckley, I.A., 2014. Change point: an R Package for change point analysis.
1228 Journal of Statistical Software 58(3), 1–19.
1229
1230 Knorn, J., Kuemmerle, T., Szabó, A., Mîndrescu, M., Keeton, W.S., Radeloff, V.C., Abrudan, I.,
1231 Griffiths, P., Gancz, V., Hostert, P., 2012. Forest restitution and the protected area effectiveness
1232 in post-socialist Romania. Biological Conservation 146 (1), 204–212.
1233
1234 Knorn, J., Kuemmerle, T., Radeloff, V.C., Keeton, W.S., Gancz, V., Biriş, I.-A., Svoboda, M.,
1235 Griffiths, P., Hagatis, A., Hostert, P., 2013. Continued loss of temperate old-growth forests in the

Romanian Carpathians despite an increasing protected area network. Environmental Conservation 40, 182–193.

Kołaczek, P., Gałka, M., Apolinarska, K., Płóciennik, M., Gąsiorowski, M., Brooks, S.J., Hutchinson, S.M., Karpińska-Kołaczek, M., 2018. A multi-proxy view of exceptionally early postglacial development of riparian woodlands with Ulmus in the Dniester River valley, western Ukraine. Review of Palaeobotany and Palynology 250, 27–43.

Kołaczek, P., Margielewski, W., Gałka, M., Karpińska-Kołaczek, M., Buczek, K., Lamentowicz, M., Borek, A., Zernitskaya, V., Marcisz, K., 2020. Towards the understanding the impact of fire on the lower montane forest in the Polish Western Carpathians during the Holocene. Quaternary Science Reviews 229, 106137

Koncek, M., 1974. Klima Tatier. Vyd. Slovenskoj Akad. Vied., Bratislava, pp. 856.

Körner, C., and Paulsen, J., 2004. A world-wide study of high altitude treeline temperatures. Journal of Biogeography 31, 713–732.

Körner, C., and Ohsawa, M., 2005. Mountain Systems. Ecosystems and Human Well-Being. Current States and Trends (ed Millennium Ecosystem Assessment), pp. 681–716. Island Press, Washington, DC, USA.

1258 Krąpiec, M., Margielewski, M., Korzeń, K., Szychowska- Krąpiec, E., Nalepka, D., Łajczak, A.,
1259 2016. Late Holocene palaeoclimate variability: The significance of bog pine dendrochronology
1260 related to peat stratigraphy. The Puścizna Wielka raised bog case study (Orwa – Norway Targ
1261 Basin, Polish Inner Carpathians). Quaternary Science Reviews 148, 192–208.
1262
1263 Kučera, P., 2012. Remarks on the intramontane continentality of the Western Carpathians
1264 defined by the absence of Fagus sylvatica. Thaiszia Journal of Botany 22 (1), 65–82.
1265
1266 Kukulak, J., 2000. Sedimentary record of early wood burning in alluvium of mountain streams in
1267 the Bieszczady range, Polish Carpathians. Palaeogeography, Palaeoclimatology, Palaeoecology
1268 164, 167–175.
1269
1270 Lévesque, M., Saurer, M., Siegwolf, R., Eilmann, B., Brang, P., Bugmann, H., Rigling, A., 2013.
1271 Drought response of five conifer species under contrasting water availability suggest high
1272 vulnerability of Norway spruce and European larch. Global Change Biology 19(10), 3184–3199.
1273
1274 Leys, B., Carcaillet, C., Blarquez, O., Lami, A., Musazzi, S., Trevisan, R., 2014. Resistance of
1275 mixed subalpine forest to fire frequency changes: the ecological function of dwarf pine (Pinus
1276 mugo ssp. mugo). Quaternary Science Reviews 90, 60–68.
1277
1278 Lindner, M., Garcia-Gonzalo, J., Kolström, M., Green, T., Reguera, R., Maroschek, M., Seidl,
1279 R., Lexer, M. J., Netherer, S., Schopf, A., Kremer, A., Delzon, S., Barbati, A., Marchetti, M.,

1280 Corona, P., 2008. Impacts of Climate Change on European Forests and Options for Adaptation.
1281 European Forest Institute, Joensuu, Finland.
1282
1283 Lung, T., Lavalle, C., Hiederer, R., Dosio, A., Bouwer, L.M., 2013. A multi-hazard regional
1284 level impact assessment for Europe combining indicators of climatic and non-climatic change.
1285 Global and Environmental Change 23, 522–536.
1286
1287 Mayewski, P.A., Rohling, E.E., Stager, C.J., Karlén, W., Maasch, K.A., Meeker, D.L.,
1288 Meyerson, E.A., Gasse, F., van Kreveld, S., Holmgren, K., Lee-Thorp, J., Rosqvist, G., Rack, F.,
1289 Staubwasser, M., Schneider, R.R., Steig, E.J., 2004. Holocene climate variability. Quaternary
1290 Research 62, 243-255.
1291
1292 Magyari, E.K., Jakab, G., Balint, M., Kern, Z., Buczko, K., Braun, M., 2012. Rapid vegetation
1293 response to lateglacial and early Holocene climatic fluctuation in the South Carpathian
1294 Mountains (Romania). Quaternary Science Reviews 35, 116–130.
1295
1296 Margielewski, W., 2006. Records of the late glacial-Holocene palaeoenvironmental changes in
1297 landslide forms and deposits of the Beskid Makowski and Beskid Wyspowy Mts. Area (polish
1298 outer Carpathians). Folia Quaternary 76, 1-149.
1299
1300 Margielewski, W., 2018. Landslide fens as a sensitive indicator of paleoenvironmental changes
1301 since the late glacial: a case study of the Polish Western Carpathians. Radiocarbon 60, 1199-
1302 1213.

1303

1304 Marlon, J.R., Bartlein, P.J., Daniau, A-L., Harrison, S.P., Maezumi, S.Y., Power, M.J., Tinner,
1305 W, Vannière, B., 2013. Global biomass burning: a synthesis and review of Holocene paleofire
1306 records and their controls. Quaternary Science Reviews 65, 5–25.

1307

1308 Meier, E.S., Lischke, H., Schmatz, D.R., Zimmermann, N.E., 2012. Climate, competition and
1309 connectivity affect future migration and ranges of European trees. Global Ecology and
1310 Biogeography 21, 164–178.

1311

1312 Miezi, P., Jakuš, R., Pennerstorfer, J., Havašová, M., Škvarenina, J., Ferenčík, J., Bičárová, S.,
1313 Bilčík, D., Blaženec, M., Netherer, S., 2017. Storms, temperature maxima and the Eurasian
1314 spruce bark beetle *Ips typographys* - An inferno trio in Norway spruce forests of the Central
1315 European High Tatra Mountains. Agricultural and Forest Meteorology 242, 85–95.

1316

1317 Noroozi, J., Talebi, A., Doostmohammadi, M., Rumpf, S.B., Peter Linder, H., Schneeweiss,
1318 G.M., 2018. Hotspots within a global biodiversity hotspot – areas of endemism are associated
1319 with high mountain ranges. Scientific Reports 8, 10345

1320

1321 Novák, J., Petr, L., Treml, V., 2010. Late Holocene human-induced changes to the extent of
1322 alpine areas in the East Sudetes, Central Europe. The Holocene 20(6), 895–905.

1323

1324 Obidowicz, A., 1996. A late glacial-Holocene history of the formation of vegetation belts in the
1325 Tatra Mountains. Acta Palaeobotanica 36(2), 159–206.

1326

1327 Ohlson, M., Brown, K.J., Birks, H.J.B., Grytnes, J.-A., Hörnberg, G., Niklasson, M., Seppä, H.,
1328 Bradshaw, R.H.W., 2011. Invasion of Norway spruce diversifies the fire regime in boreal
1329 European forests: spruce invasion alters the fire regime. Journal of Ecology 99, 395–403.
1330

1331 Oldfield, F., Wake, R., Boyle, J., Jones, R., Nolan, S., Gibbs, Z., Appleby, P., Fisher, E., Wolff,
1332 G., 2003. The late-Holocene history of Gormire Lake (NE England) and its catchment: a
1333 multiproxy reconstruction of past human impact. The Holocene 13, 677–690.
1334

1335 Pacl, J., 1973. Hydrológia Tatranského Národného Parku [Hydrology of the Tatra National
1336 Park]. Zborník Prác o TANAPe 15:181–212.
1337

1338 Pál, I., Buczkó, K., Braun, M., Vincze, I., Pálfy, J., Molnár, M., Finsinger, W., Magyari, E.K.,
1339 2016. Small-scale moisture availability increase during the 8.2 ka climatic event inferred from
1340 biotic proxy records in the South Carpathians (SE Romania). The Holocene 26, 1382–1396.
1341

1342 Pál, I., Buczkó, K, Vincze, I., Finsinger, W., Braun, M., Biró, T., Magyari, E.K., 2018.
1343 Terrestrial and aquatic ecosystem responses to early Holocene rapid climate change (RCC)
1344 events in the South Carpathian Mountains, Romania. Quaternary International 477, 79–93.
1345

1346 Panayotov, M., Gogushev, G., Tsavkov, E., Vasileva, P., Tsvetanov, N., Kulakowski, D., Bebi,
1347 P., 2017. Abiotic disturbances in Bulgarian mountain coniferous forests – An overview. Forest
1348 Ecology and Management 388, 13–28.

Pepin, N., Bradley, R., Diaz, H., Baraer, M., Caceres, E.B., Forsythe, N., Fowler, H., Greenwood, G., Hashmi, M.Z., Liu, X.D., Miller, J.R., Ning, L., Ohmura, A., Palazzi, E., Rangwala, I., Schöner, W., Severskiy, I., Shahgedanova, M., Wang, M.B., Williamson, S.N., Yang, D.Q., 2015. Elevation-dependent warming in mountain regions of the world. Nature Climate Change 5, 424–430.

Prentice, I.C., Cramer, W., Harrison, S.P., Leemans, R., Monserud, R.A., Solomon, A.M., 1992. A global biome model based on plant physiology and dominance, soil properties and climate. Journal of Biogeography 19, 117–134.

Price, M.F., Gratzer, G., Duguma, L.A., Kohler, T., Maselli, D., Romeo, R., 2011. Mountain Forests in a Changing World – Realizing Values, Addressing Challenges. FAO/MPS and SDC, Rome, Italy.

Punt, W., 1976–1996. The Northwest European Pollen flora 1–7. Elsevier, Amsterdam.

Reimer, P.J., Bard, E., Bayliss, A., Beck, J.W., Blackwell, P.G., Ramsey, C.B., Buck, C.E., Cheng, H., Edwards, R.L., Friedrich, M., Grootes, P.M., Guilderson, T.P., Haflidason, H., Hajdas, I., Hatté, C., Heaton, T.J., Hoffmann, D.L., Hogg, A.G., Hughen, K.A., Kaiser, K.F., Kromer, B., Manning, S.W., Niu, M., Reimer, R.W., Richards, D.A., Scott, E.M., Southon, J.R., Staff, R.A., Turney, C.S.M., van der Plicht, J., 2013. IntCal13 and Marine13 radiocarbon age calibration curves 0–50,000 years cal BP. Radiocarbon 55(4), 1869–1887.

Renberg, I., Brännvall, M-L., Bindler, R., Emteryd, O., 2000. Atmospheric lead pollution history during four millennia (2000 BC to 2000 AD) in Sweden. Ambio 29(3), 150–156.

Rybníčková, E., and Rybníček, K., 2006. Pollen and macroscopic analyses of sediments from two lakes in the High Tatra Mountains, Slovakia. Vegetation History and Archaeobotany 15, 345–356.

Schaffer, J., and Stummer, F., 1933. Atlas der Seen der Hohen Tatra, III. Geographisches Institut der Deutschen Universität Prag. Blätter Popper See und Tschirmer See.

Schillereff, D. N., Chiverrell, R. C., Macdonald, N., Hooke, J. M., 2014. Flood stratigraphies in lake sediments: A review. Earth Science Reviews 135, 17–37.

Schillereff, D. N., Chiverrell, R. C., Macdonald, N., Hooke, J., Welsh, K. E., Piliposian, G., Croudace, I. W., 2019. Convergent human and climate forcing of late-Holocene flooding in Northwest England. Global and Planetary Change, 182, 102998.

Schneider, C.A., Rasband, W.S., Eliceiri, K.W., 2012. NIH Image to ImageJ: 25 years of image analysis. Nature Methods 9, 671–675.

1393 Schnitchen, C., Charman, D.J., Magyari, E., Braun, M., Grigorszky, I., Tóthmérész, B., Molnár,
1394 M., Szántó, Z., 2006. Reconstructing hydrological variability from testate amoebae analysis in
1395 Carpathian peatlands. Journal of Paleolimnology 36, 1–17.
1396
1397 Schumacher, S., Bugmann, H., 2006. The relative importance of climatic effects, wildfires and
1398 management for future forest landscape dynamics in the Swiss Alps. Global Change Biology 12,
1399 1435–1450.
1400
1401 Schumacher, M., Schier, W., Schütt, B., 2016. Mid-Holocene vegetation development and
1402 herding-related interferences in the Carpathian region. Quaternary International 415, 253–267.
1403
1404 Schwörer, C., Colombaroli, D., Kaltenrieder, P., Rey, F., Tinner, W., 2015. Early human impact
1405 (5000–3000 BC) affects mountain forest dynamics in the Alps. Journal of Ecology 103, 281–
1406 295.

1407 Seidl, R., Schelhaas, M.-J., Rammer, W., Verkerk, P.J., 2014. Increasing forest disturbances in
1408 Europe and their impact on carbon storage. Nature Climate Change 4, 806–810.

1409 Šolcová, A., Hájková, P., Petřík, J., Tóth, P., Rohovec, J., Bátora, J., Horsák, M., 2018. Early and
1410 middle Holocene ecosystem changes at the Western Carpathian/Pannonian border driven by
1411 climate and Neolithic impact. Boreas 47(3), 897–909.

1412 Stähli, M., Finsinger, W., Tinner, W., Allgöwer, B., 2006. Wildland fire history and fire ecology
1413 of the Swiss National Park (Central Alps): New evidence from charcoal, pollen and plant
1414 macrofossils. The Holocene 16, 805–817.

Starkel, L., Michczyńska, D., Krąpiec, M., Margielewski, W., Nalepka, D., Pazdur, A., 2013. Progress in the Holocene chrono- climatostratigraphy of Polish territory. Geochronometria. 40(1), 1–21.

Stockmarr, J., 1972. Tablets with spores used in absolute pollen analysis. Pollen and Spores 13, 614–621.

Tanţău, I., Feurdean, A., de Beaulieu, J.L., Reille, M., Fărcaş, S., 2011. Holocene vegetation history in the upper forest belt of the Eastern Romanian Carpathians. Palaeogeography, Palaeoclimatology, Palaeoecology 309, 281–290.

Temperli, C., Bugmann, H., Elkin, C., 2013. Cross-scale interactions among bark beetles, climate change, and wind disturbances: a landscape modeling approach. Ecological Monographs 83, 383–402.

Tinner, W., 2007. Treeline studies, in: Elias, S.A. (Ed.), Encyclopedia of Quaternary Science. Elsevier B.V., Amsterdam, The Netherlands, pp. 2374–2384.

Tomlinson, P., 1985. An aid to the identification of fossil buds, bud-scales and catkin-bracts of British trees and shrubs. Circaea 3, 45–130.

Topographic maps of Romania, 1986. 1:25000.

1438

1439 Tóth, M., Magyari, E.K., Buczkó, K., Braun, M., Panagiotopoulos, K., Heiri, O., 2015.
1440 Chironomid-inferred Holocene temperature changes in the southern Carpathians (Romania). The
1441 Holocene 25, 569–582.

1442

1443 Troels-Smith, J., 1955. Karakterisering af løse jordarter. Geological Survey of Denmark,
1444 Copenhagen. pp. 1–73.

1445

1446 Trondman, A.-K., Gaillard, M.-J., Mazier, F., Sugita, S., Fyfe, R., Nielsen, A.B., Twiddle, C.,
1447 Barratt, P., Birks, H.J.B., Bjune, A.E., Björkman, L., Broström, A., Caseldine, C., David, R.,
1448 Dodson, J., Dörfler, W., Fischer, E., van Geel, B., Giesecke, T., Hultberg, T., Kalnina, L.,
1449 Kangur, M., van der Knaap, P., Koff, T., Kuneš, P., Lagerås, P., Latałowa, M., Lechterbeck, J.,
1450 Leroyer, C., Leydet, M., Lindbladh, M., Marquer, L., Mitchell, F.J.G., Odgaard, B.V., Peglar,
1451 S.M., Persson, T., Poska, A., Rösch, M., Seppä, H., Veski, S., Wick, L., 2015. Pollen-based
1452 quantitative reconstructions of Holocene regional vegetation cover (plant-functional types and
1453 land-cover types) in Europe suitable for climate modelling. Global Change Biology 21, 676–697.

1454

1455 UNEP, 2007. Carpathians Environmental Outlook. United Nations Environment Programme
1456 UNEP). Geneva, Switzerland, pp. 236.

1457

1458 UNESCO-WNBR. http://www.unesco.org/new/en/natural-sciences/environment/ecological-
1459 sciences/biosphere-reserves/europe-north-america/polandslovakia/tatra/. Accessed April 29,
1460 2020.

Valde-Nowak, P., and Soják, M., 2010. Contribution to the Mesolithic in the Slovak Carpathians. Slovenská Archeológia, 58, 1–12.

Vannière, B., Blarquez, O., Rius, D., Doyen, E., Brücher, T., Colombaroli, D., Connor, S., Feurdean, A., Hickler, T., Kaltenrieder, C., Leys, B., Massa, C., Olofsson, J., 2016. 7000-year human legacy of elevation-dependent European fire regimes. Quaternary Science Reviews 132, 206–212.

Vincze, I., Orbán, I., Birks, H.H., Pál, I., Finsinger, W., Hubay, K., Marinova, E., Jakab, G., Braun, M., Biró, T., Tóth, M., Dănău, C., Ferencz, I.V., Magyari, E.K., 2017. Holocene treeline and timberline changes in the South Carpathians (Romania): Climatic and anthropogenic drivers on the southern slopes of the Retezat Mountains. The Holocene 27(11), 1613–1630.

Walther GR., Beißner S., Pott R., 2005. Climate Change and High Mountain Vegetation Shifts. In: Broll G., Keplin B. (eds) Mountain Ecosystems. Springer, Berlin, Heidelberg.

Werners, S.E., Bos, E., Civic, K., Hlásny, T., Hulea, O., Jones-Walters, L., Kőpataki, E., Kovbasko, A., Moors, E., Nieuwenhuis, E., van de Velde, I., Zingstra, H., Zsuffa, I., 2014. Climate change vulnerability and ecosystem-based adaptation measures in the Carpathian region: Final Report - Integrated assessment of vulnerability of environmental resources and ecosystem-based adaptation measures. Wageningen, Alterra Wageningen UR (University & Research centre), Alterra report 2572. 132 pp.

Wood, S.N., 2017. Generalized Additive Models: An Introduction with R (2nd edition). Chapman and Hall/CRC. pp 1–476.

Zasadni, J. and Kłapyta, P., 2014. The Tatra Mountains during the Last Glacial Maximum. Journal of Maps 10 (3), 440–456.